Chapter 8

Synthesis and Physical Properties of Red Luminescent Glass Forming Pyranylidene and Isophorene Fragment Containing Derivatives

Elmars Zarins, Aivars Vembris, Valdis Kokars and Inta Muzikante

Additional information is available at the end of the chapter

http://dx.doi.org/10.5772/53462

1. Introduction

Low molecular mass organic compounds with internal charge transfer properties are widely adopted for organic photonics such as materials for the creation of molecular electronics elements, organic magnets, solar cells and organic light emitting diodes (OLEDs) for full display panels [1-3]. One of the most widely used red light-emitting materials contains pyranylidene (4*H*-pyran-4-ylidene) or isophorene (5,5-dimethylcyclohex-2-enylidene) fragments as backbone of the molecule (see Fig.1), which are conjugated in a system with electron acceptor and electron donor fragments [1,4-24]. In many cases the light-emitting layer from such commercially available compounds is prepared by thermal evaporation in vacuum [1-2, 25-27]. Some of them are used as dopants in a polymer matrix and spin-coated onto a hole transport layer from solution [1,12]. However the doping amount of luminescent compound is limited by self crystallization and photoluminescence quenching at higher concentrations which reduce the quantum efficiency of fabricated devices significantly [11-12]. Therefore it is important to synthesize low molecular mass light-emitting organic compounds which do not crystallize and form thin amorphous solid films from volatile organic solvents. Such compounds, which can make a solid-state glassy structure prepared from solutions, could facilitate technological processes in the production of many devices in optoelectronics, for example, light emitting devices by low-cost deposition such as wet casting methods and easier light-emitting material synthesis. Some of these red light-emitting compounds have been introduced by us [28-32].

In this chapter we present complete synthesis, thermal, optical, photoelectrical and glass forming properties of new organic glass-forming pyranylidene and isophorene fragment containing derivatives with bulky trityloxy groups in their molecules. The optical properties, both in solution and solid state, are compared. The dependance of

photoelectrical properties and energy structure of glassy films on molecular structure will be discussed. The most popular derivatives of pyranylidene and isophorene used in OLEDs are shown in Fig.1.

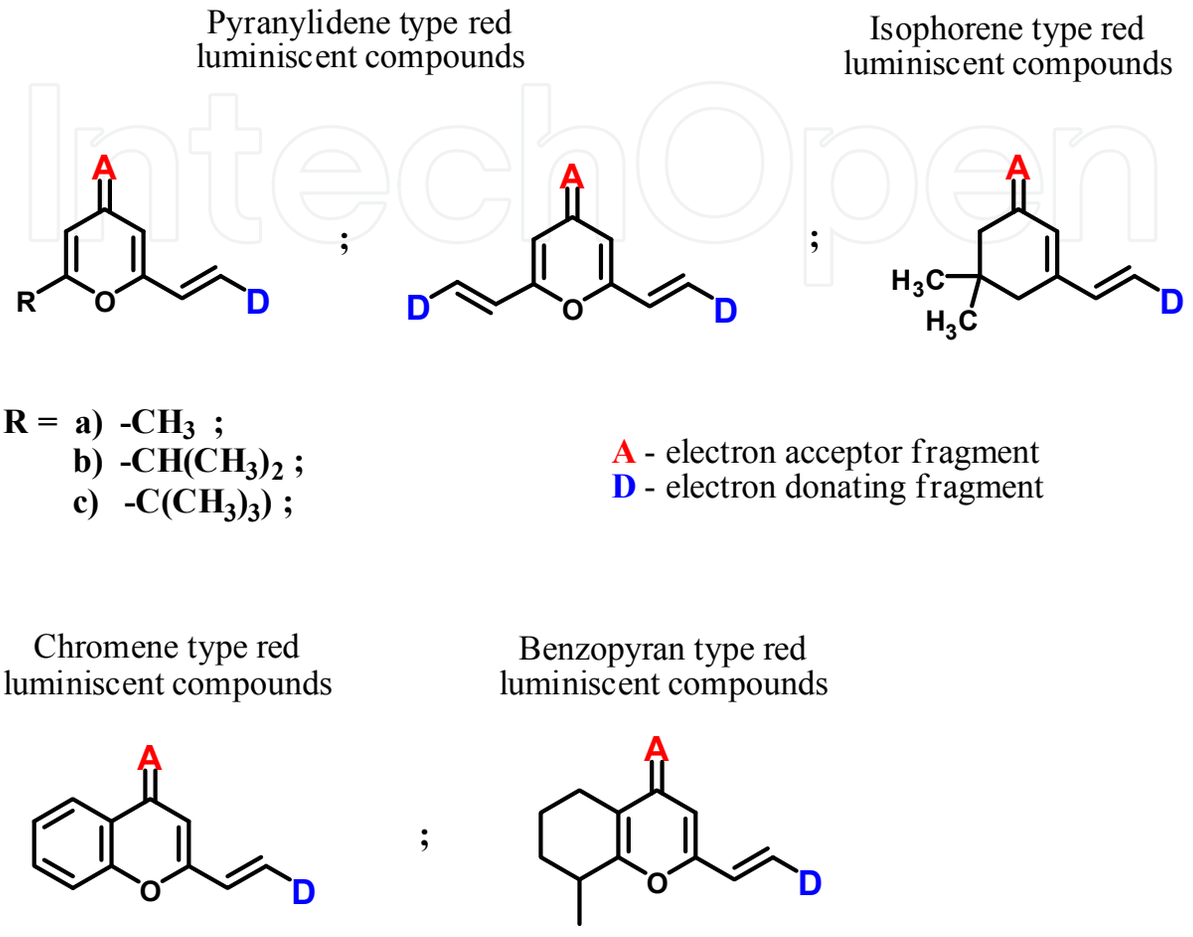

Figure 1. Most widely used pyranylidene and isophorene type red-emitters used as OLED emission layer materials

2. Synthesis

The synthesis procedure of pyranylidene and isophorene D-π-A type luminophores (see Fig.1) with either one or two electron donor fragments can be divided into three main parts:

1. Synthesis of a backbone fragment: Synthesis of derivatives of 4*H*-pyran-4-one, which in their molecules contain not only a carbonyl group, but also at least one methyl group and are able to react further with aromatic aldehydes.
2. Addition of an electron acceptor fragment to the backbone: Condensation reaction of 4*H*-pyran-4-one derivatives synthesized in 1) with active methylene group containing compounds.
3. Synthesis of pyranylidene and isophrene D-π-A type red emitters: Final addition of electron donor group containing aromatic aldehydes to compounds obtained in 2).

2.1. Synthesis of the backbone fragment: 2,6-disubstituted-4*H*-pyran-4-ones

The simplest of 2,6-disubstituted-4*H*-pyran-4-ones is 2,6-dimethyl-4*H*-pyran-4-one (compound 2 in Fig.2), which is obtained in 86% yield from dehydroacetic acid (compound 1 in Fig.2) by acidic rearrangement with following decarboxylation (see Fig.2) [32-33].

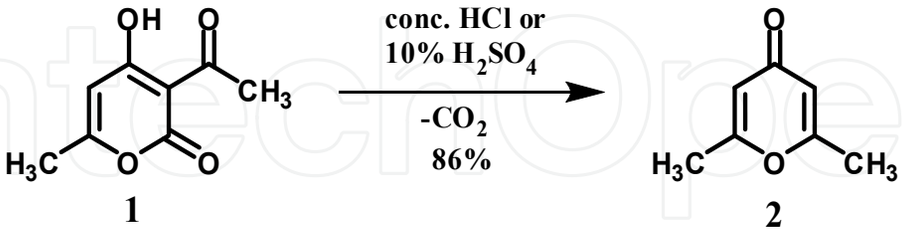

Figure 2. Synthesis of 2,6-dimethyl-4*H*-pyran-4-one. Dehydroacetic acid (compound **1**) is suspended either in concentrated hidrochloric acid (conc. HCl) or 10% aqueous sulfuric acid (10% H_2SO_4) and heated. During the heating carbon dioxide (CO_2) is liberated and 2,6-dimethyl-4*H*-pyran-4-one (compound **2**) is formed.

2,6-Dimethyl-4*H*-pyran-4-one (compound **2** in Fig.2) has one carbonyl group which can further react with active methylene group containing compounds in *Knoevenagel* condensation reactions. It also has two activated methyl groups, which can react in the same type of condensation reactions with one or two molecules of aromatic aldehydes.

Another method for the syntheis of 2,6-disubstituted-4*H*-pyran-4-ones, which contain at least one active methyl group, is using 4-hydroxy-6-methyl-2*H*-pyran-2-one (compound **3** in Fig.3) as starting material [11,34]. Its further reaction with isobutyryl chloride (compound **4** in Fig.3) in trifluoroacetic acid (TFA) gives 6-methyl-2-oxo-2*H*-pyran-4-yl isobutyrate (compound **5** in Fig.3). Without separating the compound **5** from the reaction mixture it was subjected to *Fries rearrangement* resulting in 4-hydroxy-3-isobutyryl-6-methyl-2*H*-pyran-2-one (compound **6** in Fig.3). In its decarboxylation and further acidic cyclization reactions 2-isopropyl-6-methyl-4*H*-pyran-4-one (compound **8** in Fig.3) is obtained with 80% yield. Compound **8** also contains a carbonyl group, just as the previously synthesized 2,6-dimethyl-4*H*-pyran-4-one (compound **2** in Fig.2). Since it now contains just one activated methyl group, only one aromatic aldehyde containing fragment can be added to the **backbone** of pyranylidene derivative **8** (shown in Fig.3).

One of the most preferred 2,6-disubstituted-4*H*-pyran-4-ones is 2-*tert*-butyl-6-methyl-4*H*-pyran-4-one (compound **13** in Fig.4) [7,11,35]. The first synthesis method starts from 3,3-dimethylbutan-2-one (compound **9** in Fig.4). Treating it with acetic anhydryde (Ac_2O) and boron trifluoride (BF_3) a boron enolate (compound **10** in Fig.4) is obtained. Its further condensation reaction with 1,1-dimethoxy-N,N-dimethylethanamine (compound **11** in Fig.4) produces N,N-dimethylamino-vinyl group containing boron enolate (compound **12** in Fig.4). Then following an acidic treatment gives 2-*tert*-butyl-6-methyl-4*H*-pyran-4-one (compound **13** in Fig.4). However this method has a drawback because two synthetic reactions towards our target compound had low yields (30-40%), which results in a very low overall yield for synthesis of 2-*tert*-butyl-6-methyl-4*H*-pyran-4-one (compound **13** in Fig.4).

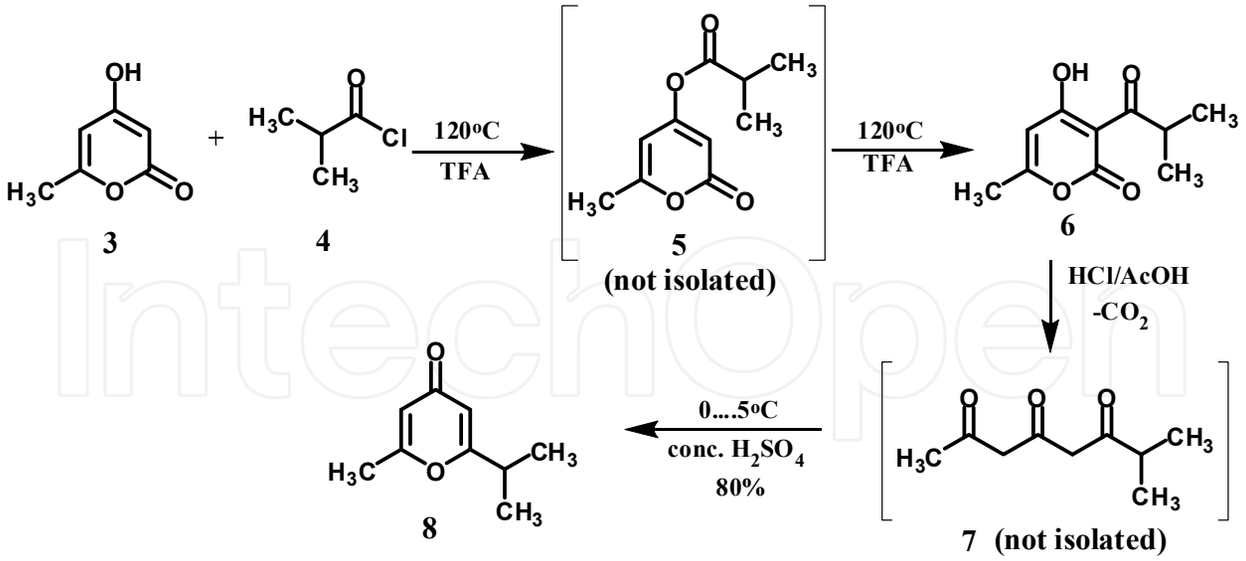

Figure 3. Synthesis of 2-isopropyl-6-methyl-4*H*-pyran-4-one (compound **8**). TFA - trifluoroacetic acid, HCl - hidrochloric acid, AcOH - acetic acid, CO_2 - carbon dioxide, conc. H_2SO_4 - concentrated sulfuric acid.

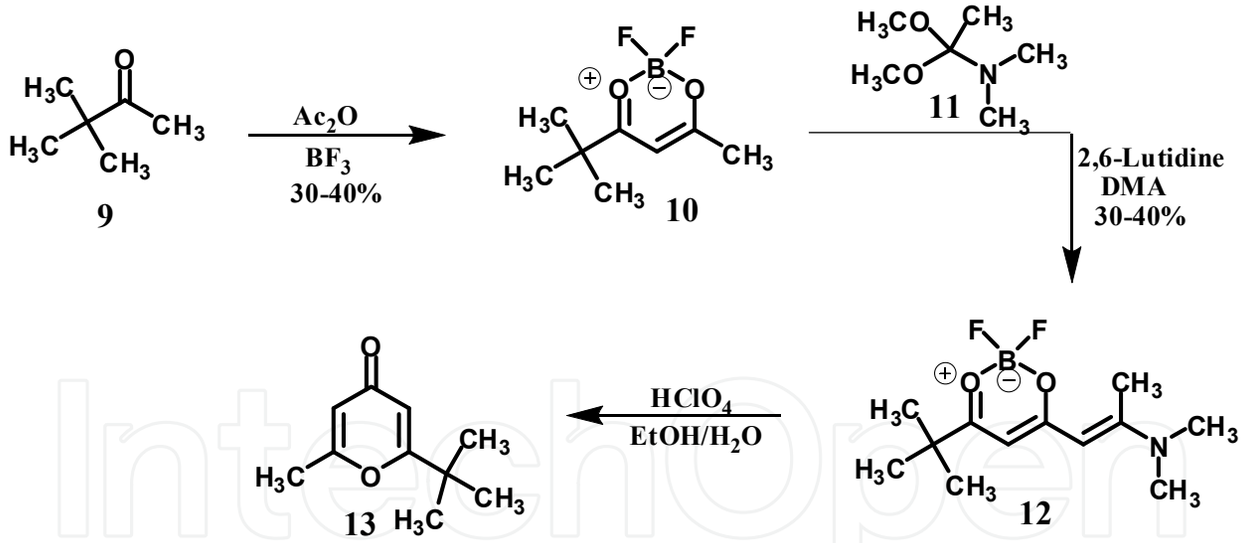

Figure 4. Conventional synthesis of 2-*tert*-butyl-6-methyl-4*H*-pyran-4-one (compound **13**). Ac_2O - acetic anydryde, BF_3 - bornon trifluoride, DMA - dimethylamine, $HClO_4$ - perchloric acid, EtOH - ethanol.

Fortunately, there is another method for synthesizing 2-*tert*-butyl-6-methyl-4*H*-pyran-4-one (compound **13** in Fig.4) with good yields [7] using pentane-2,4-dione (compound **14** in Fig.5) as starting reactant.

In its *Aldol reaction* with methyl pivalate (compound **15** in Fig.5) a 7,7-dimethyloctane-2,4,6-trione (compound **16** in Fig.5) was formed. Without separating the compound **16** from reaction mixture it was subjected to acidic cyclization producing 2-*tert*-butyl-6-methyl-4*H*-

pyran-4-one (compound **13** in Fig.5) with a good overall yield (60%). As with 2-isopropyl-6-methyl-4*H*-pyran-4-one (compound **8** in Fig.3), the resulting 2-*tert*-butyl-6-methyl-4*H*-pyran-4-one (compound **13** in Fig.5) also contains one carbonyl group and one activated methyl group with the possibility of also adding **only one** aromatic aldehyde containing fragment.

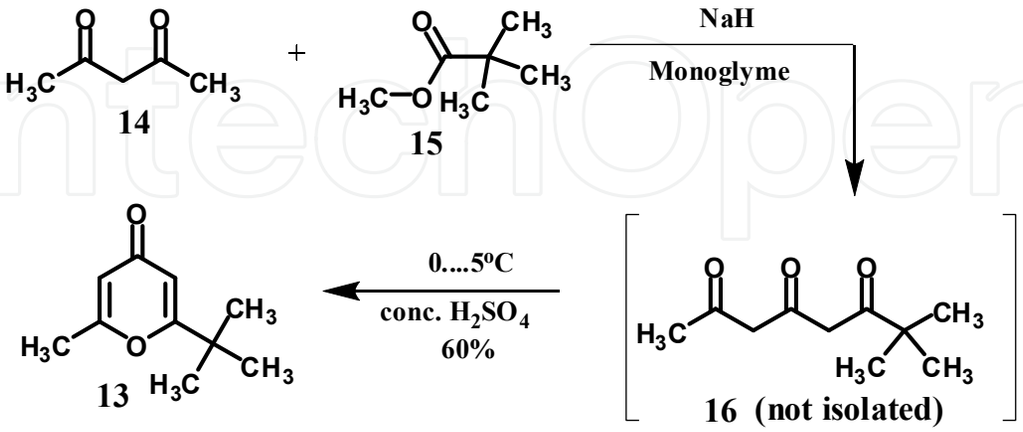

Figure 5. Improved synthesis of 2-*tert*-butyl-6-methyl-4*H*-pyran-4-one (compound **13**). NaH - sodium hydryde, conc. H_2SO_4 - concentrated sulfuric acid.

One of oldest, but no less important methods known for the synthesis of 2,6-disubstituted-4*H*-pyran-4-ones is to obtain them from 3-substituted-vinylcarbonyl-4-hydroxy-6-methyl-2*H*-pyran-2-ones (compounds **17** in Fig.6) [33]. Compounds **17** are obtained from dehydroacetic acid (compound **1** in Fig.6), in which the methyl group in the acetyl fragment is activated to react preferentially with aromatic aldehydes (see Fig.6) giving 3-substituted-vinylcarbonyl-4-hydroxy-6-methyl-2*H*-pyran-2-ones (compounds **17** in Fig.6) [33, 36]. Details on the obtained compounds **17** and their dependence on substituents (R) in their molecules are given in Table 1. They serve as precursors for further synthesis of pyranylidene type compounds.

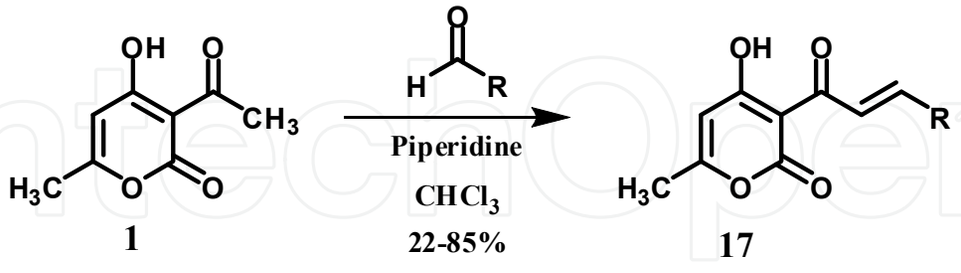

Figure 6. Synthesis of 3-substituted-vinylcarbonyl-4-hydroxy-6-methyl-2*H*-pyran-2-ones (Compounds **17**). Above the arrow are different aromatic aldehydes with different substituents R (see Table 1), which all react with dehydroacetic acid (compound **1**) the same way. $CHCl_3$ - chloroform.

Using this approach it is possible to obtain many different mono-styryl-substituted 4*H*-pyran-4-ones (compounds **17** in Fig.7). However only a few of previously synthesized compounds **17** give 2-styryl-substituted-6-methyl-4*H*-pyran-4-ones (compounds **18** in Fig.7) by acidic decarboxylation under the reaction conditions reported in [30, 33] (see Fig.7) as summarised in Table 2.

R (of compounds 17)	Yield, %	M.p., °C	Recrystallized from
Phenyl	55	130-132	methanol
o-Nitrophenyl	65	161-163	acetic acid/water
m-Nitrophenyl	60	192	chloroform
p-Nitrophenyl	22	165-167	chloroform/ethyl acetate
p-Nitrophenyl	47	246-247	dioxane
p-Dimethylaminophenyl	71	198-200	Chloroform, ethyl acetate, benzene
p-Diethylaminophenyl	58	150	Chloroform, ethyl acetate
o-Hydroxyphenyl	67	186-188	methanol
m-Hydroxyphenyl	61	181-183	ethanol
p-Hydroxyphenyl	69	260-262	dioxane
p-Methoxyphenyl	73	153-154	ethanol
2,3-Dimethoxyphenyl	47	147	ethyl acetate
3,4-Dimetoxyphenyl	46	185	benzene/ethyl acetate
3,4-Diethoxyphenyl	43	163	ethyl acetate
o-Chlorophenyl	36	116-117	ethanol
p-Chlorophenyl	54	155-156	ethanol
3,4-Dichlorophenyl	46	185	ethyl acetate, benzene/chloroform
p-Isopropylphenyl	65	139-141	methanol
1-Naphtyl	62	190	ethyl acetate
β-styryl	57	185	chloroform/ethyl acetate
2-Furyl	85	144	benzene/ethyl acetate

R - substituents of aromatic aldehydes which also remain in the structure of compounds **17** after reactions.
Yield - the practical production of the particular compound **17** in the reaction of dehydroacetic acid (compound **1** in Fig.6) with the corresponding aromatic aldehyde. M.p. - melting point of the particular compound **17**. Recrystallized from - organic solvent, which is used for the particular compound **17** final purification.

Table 1. Synthetic information on pyranylidene compounds **17** (see Fig.6).

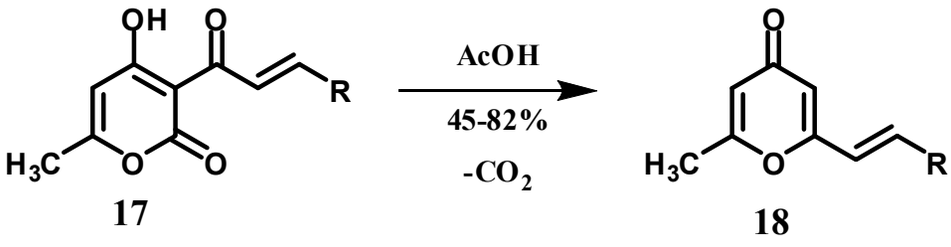

Figure 7. Synthesis of 2-styryl-substituted-6-methyl-4*H*-pyran-4-ones (compounds **18**).

R (of compounds 18)	**Yield, %**	**M.p., °C**	**Recrystallized from**
p-Dimethylaminophenyl	82	156	ethyl acetale/petroleum ether
p-Diethylaminophenyl	68	128-130	methanol/water
o-Nitrophenyl	53	187-189	methanol/water
p-Isopropylphenyl	45	110-112	ethanol/water

R - substituents of aromatic aldehydes which also remain in the structure of compounds **17** after reactions.
Yield - the practical production of the particular compound **17** in the reaction of dehydroacetic acid (compound **1** in Fig.6) with the corresponding aromatic aldehyde. M.p. - melting point of the particular compound **17**. Recrystallized from - organic solvent, which is used for the particular compound **17** final purification.

Table 2. Fries rearrangement possibility [33] of pyranylidene precursors **17** (Fig.7).

Some works can be found on red luminescent compounds where the pyranylidene fragment is hidden as a substructure in the molecule [8, 23-24]. For example, chromene type derivatives of pyranylidene are synthesized from 1-(2-hydroxyphenyl)ethanone (compound **19** in Fig.8) [23-24]. In the *Claisen condensation* reaction (see Fig.8) with ethyl-acetate in the presence of a strong base, 1-(2-hydroxyphenyl)butane-1,3-dione (compound **20** in Fig.8) is obtained. After separation it was subjected to acidic dehydrocyclization giving 2-methyl-4*H*-chromen-4-one (compound **21** in Fig.8) with an overall 45% yield.

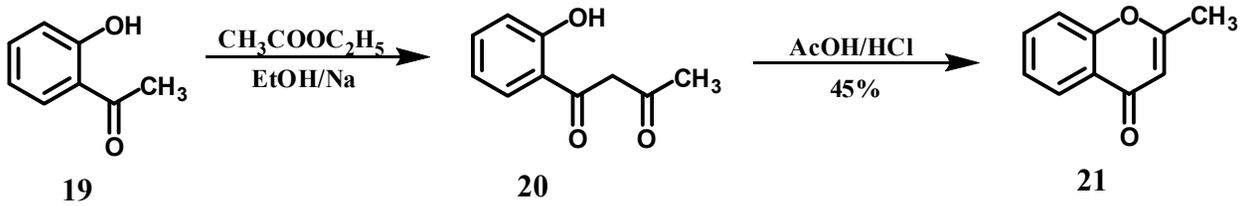

Figure 8. Synthesis of chromene fragment containing derivative of pyranylidene (compound **21**).

For obtaining the benzopyran derivative of pyranylidene [8, 24], a two-stage synthesis procedure is started from 2-methylcyclohexanone (compound **22** in Fig.9).

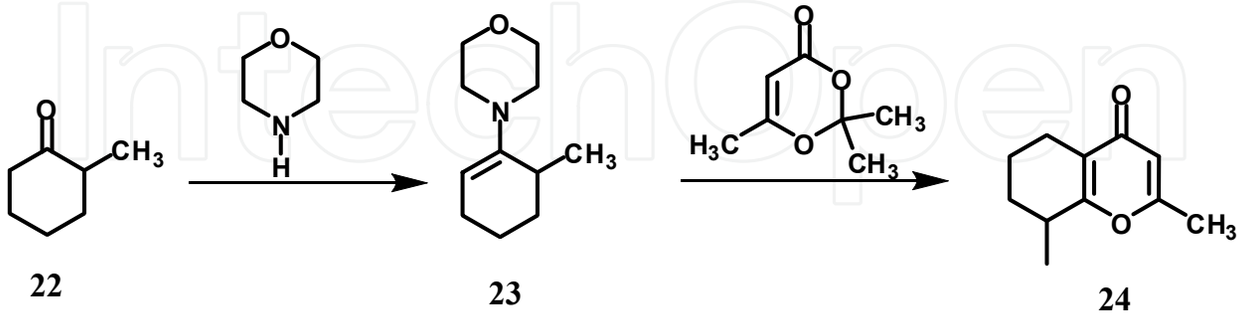

Figure 9. Synthesis of the benzopyran fragment containing derivative of pyranylidene (compounds **24**).

In the first stage of synthesis, treatment with morpholine gives us enamine **23** (4-(6-methylcyclohex-1-enyl)morpholine). In the second stage of synthesis in reaction with 2,2,6-trimethyl-4*H*-1,3-dioxin-4-one, a 2,8-dimethyl-5,6,7,8-tetrahydro-4*H*-chromen-4-one (compound **24** in Fig.9) is sucessfully obtained. Once the desired pyranylidene compound is

obtained, the addition of electron acceptor and electron donor fragments becomes a more simplified process, which will be described in detail below in this chapter.

2.2. Addition of electron acceptor fragments to derivatives of 4*H*-pyran-4-ones and 3,5,5-trimethylcyclohex-2-enone

The next step towards synthesizing fully functional pyranilydene and isophorene type red luminescent organic compounds is the addition of electron acceptor fragments to the previously obtained 2,6-disubstituted-4*H*-pyran-4-ones (see Fig.10) and 3,5,5-trimethylcyclohex-2-enone (see Fig.11).

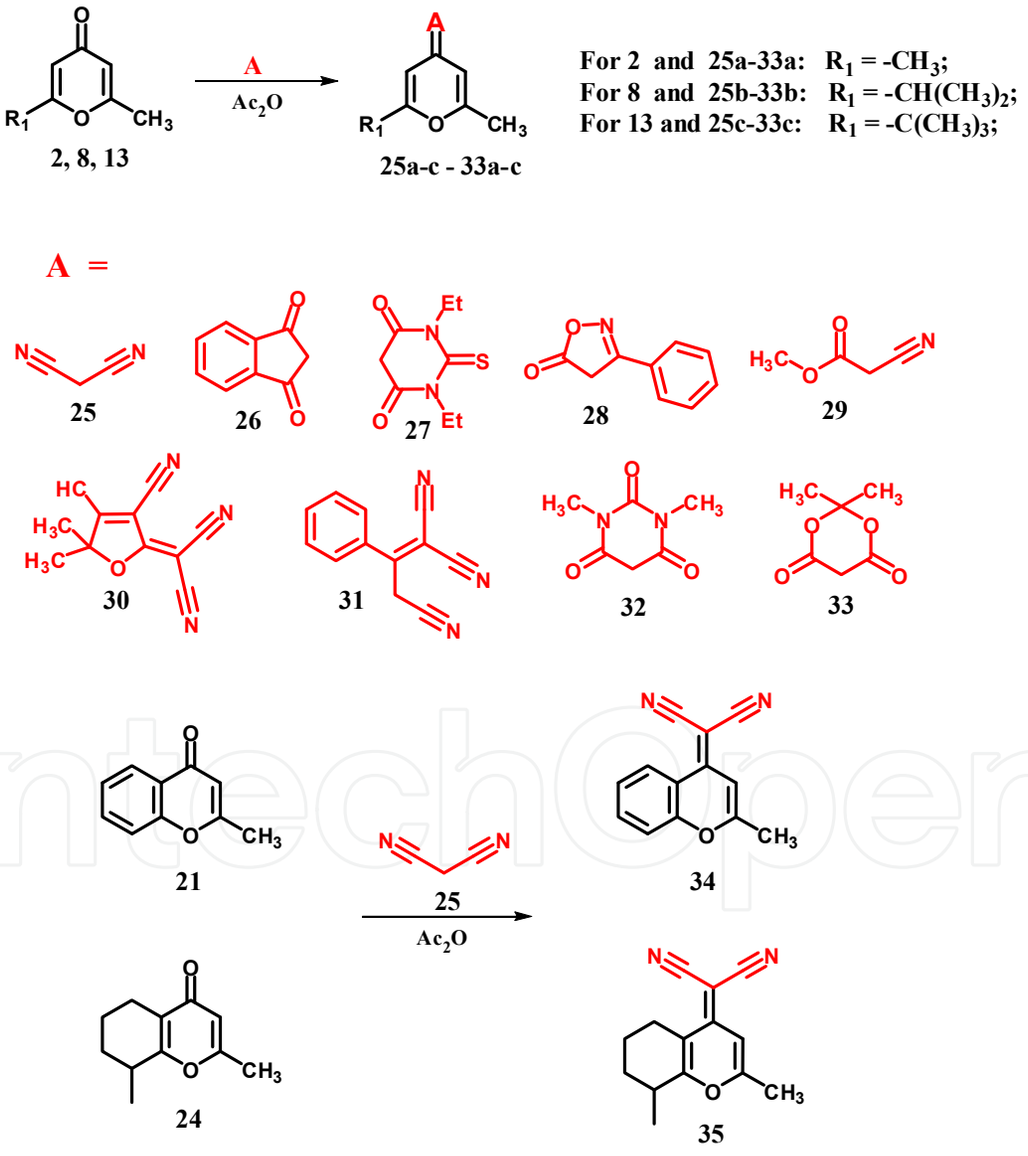

Figure 10. Synthesis of electron acceptor fragment containing derivatives of pyranylidene. Electron acceptors are marked in red while structure backbone, which serves as π-conjugated system remain in black.

Many different electron acceptor fragments (compounds **25-35** in Fig.10) can be introduced in 2,6-disubstituted-4*H*-pyran-4-ones [1,4-18, 28-30,32] using acetic anhydride (Ac_2O) as solvent and catalyst. From these, malononitrile (compounds **25** in Fig.10) is the most commonly used. Since isophorene (3,5,5-trimethylcyclohex-2-enone) (compound **36** in Fig.11) is an inexpensive reagent, which can be purchased from chemical suppliers - such as ACROS and ALDRICH, all that remains is to add electron acceptor and electron donor fragments. As with 2,6-disubstituted-4*H*-pyran-4-ones, the electron acceptor fragments are added in *Knoevenagel* condensation reactions [18-21, 31, 37] with active methylene group containing compounds **37-39** (see Fig.11).

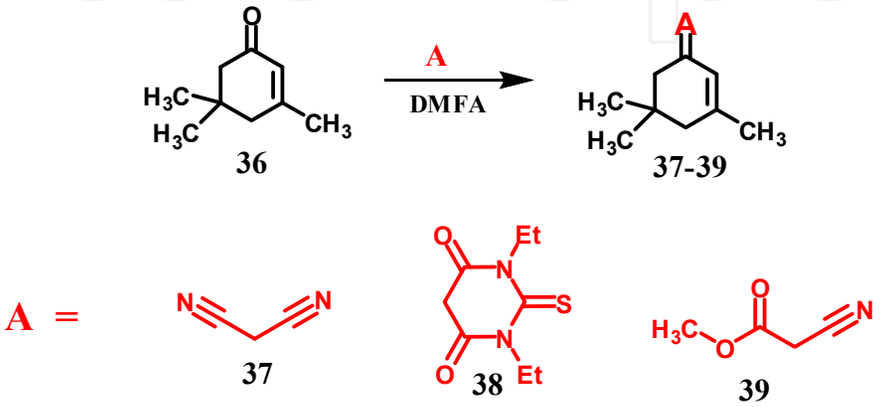

Figure 11. Synthesis of electron acceptor fragment containing derivatives of isophorene (compounds 37-39). As in Figure 10, the electron acceptors are marked in red while the structure backbone remains in black.

The electron acceptor fragment containing derivatives of isophorene (3,5,5-trimethylcyclohex-2-enone) (compounds **37-39** in Fig.11) thus obtained are not always isolated from the reaction mixture [31, 37]. Once they are formed, the electron donor fragment containing aromatic aldehyde is added in the mixture for further reaction with the aldehyde.

2.3. Synthesis of pyranilydene and isophorene type red luminescent compounds by final addition of electron donor fragments

Once the electron acceptor fragment is introduced, the last step for obtaining a fully functional pyranylidene and isophorene red luminescent compounds is to add one or two electron donor fragment containing aldehydes. They are added in *Knoevenagel* condensation reactions with electron acceptor fragment containing derivatives of isophorene as shown in Fig.12 and pyranylidene shown in Fig.13, which contain one or two activated methyl groups.

For isophorene type compounds one electron donor fragment (**40-44**) is always introduced after an electron acceptor fragment is already in the molecule (see Fig.12) [18-21, 31, 37]. Many different structures of electron donor fragments are introduced (compounds **45-57** in Fig.13) in the pyranylidene backbone after introducing the electron acceptor fragment [1,4-18,27-29,31]. In cases where only one methyl group reacts with the aldehyde, a mono-styryl

derivative of pyranylidene is obtained (see Fig.13). However, as all possible combinations shown in Fig.13 have not yet been synthesized, it presents a working opportunity for many organic chemists to contribute. If a pyranylidene type compound has two active methyl groups, like compound **25a**, (see Fig.10) it will react with one or two aromatic aldehyde molecules producing chromophores **58-66** (see Fig.14). The reaction product will most likely be a mixture of mono- and bis- condensation products, which are difficult to separate and purify [32]. In reaction with two methyl groups bis-styryl derivatives of pyranylidene are obtained (see Fig.14).

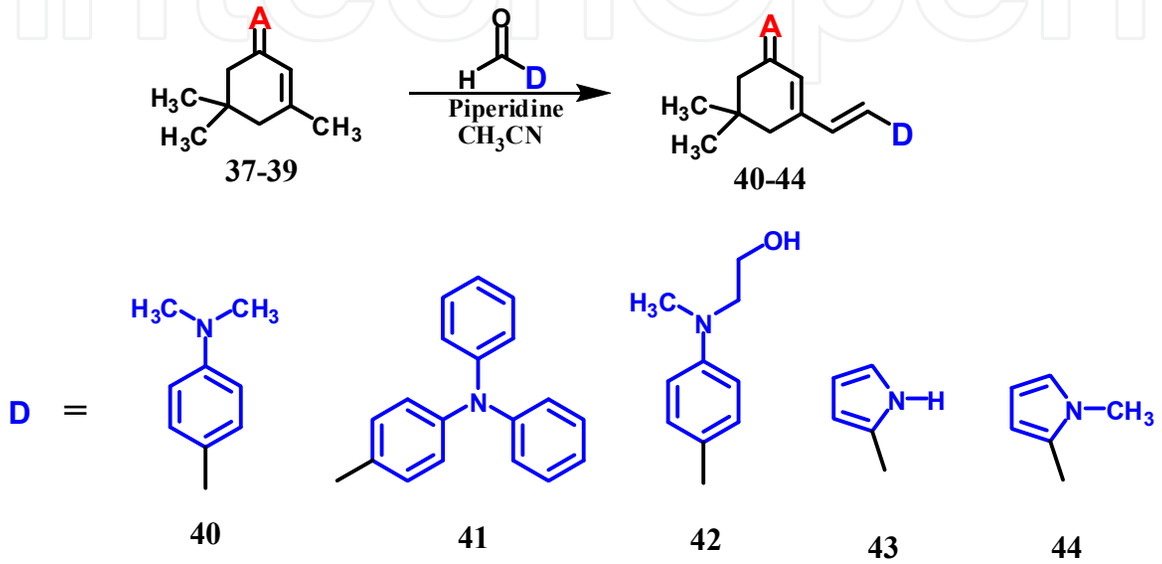

Figure 12. Synthesis of fully functional derivatives of isophorene (compounds **40-44**). CH_3CN - acetonitrile. Electron acceptor fragments are marked in red and electron donor fragments are marked in blue, while the backbone structure fragments remain in black and serve as a π-conjugated system.

A good summary on dicyanomethylene-pyranylidene type red-emitters has been made by Guo et al. [24], according to which the mono electron donor fragment containing pyranylidene-type materials (**45a-c** to **57a-c** in Fig.13) usually have high luminescence quantum yield but their chromaticity is not sufficiently good. At the same time two electron donor fragment derivatives of pyranylidene (compounds **58-66** in Fig.14) have better chromaticity, but their luminance efficiency is relatively low, particulary those with larger conjugations leading to a broad light-emission peak above 650 nm extending to the NIR region, which decreases the efficiency of red electroluminescent materials.

Both chromene (compounds **47,49-50** in Fig.13) and benzopyran (compounds **47,49,51** in Fig.13) type derivatives of pyranylidene have only one electron donor fragment in their molecules, but their optical properties are different. Since chromene type derivatives of pyranylidene have an additional conjugated aromatic ring in its molecule, its optical properties are similar to those with two electron donor fragment derivatives of pyranylidene (compounds **58-66** in Fig.14). At the same time benzopyran pyranylidene compounds **45,46,49** have a simple cyclohexene ring without additional conjugation, so their optical properties are more similar to pyranylidene-type red-emitters, compounds **45a-c** to **57a-c**.

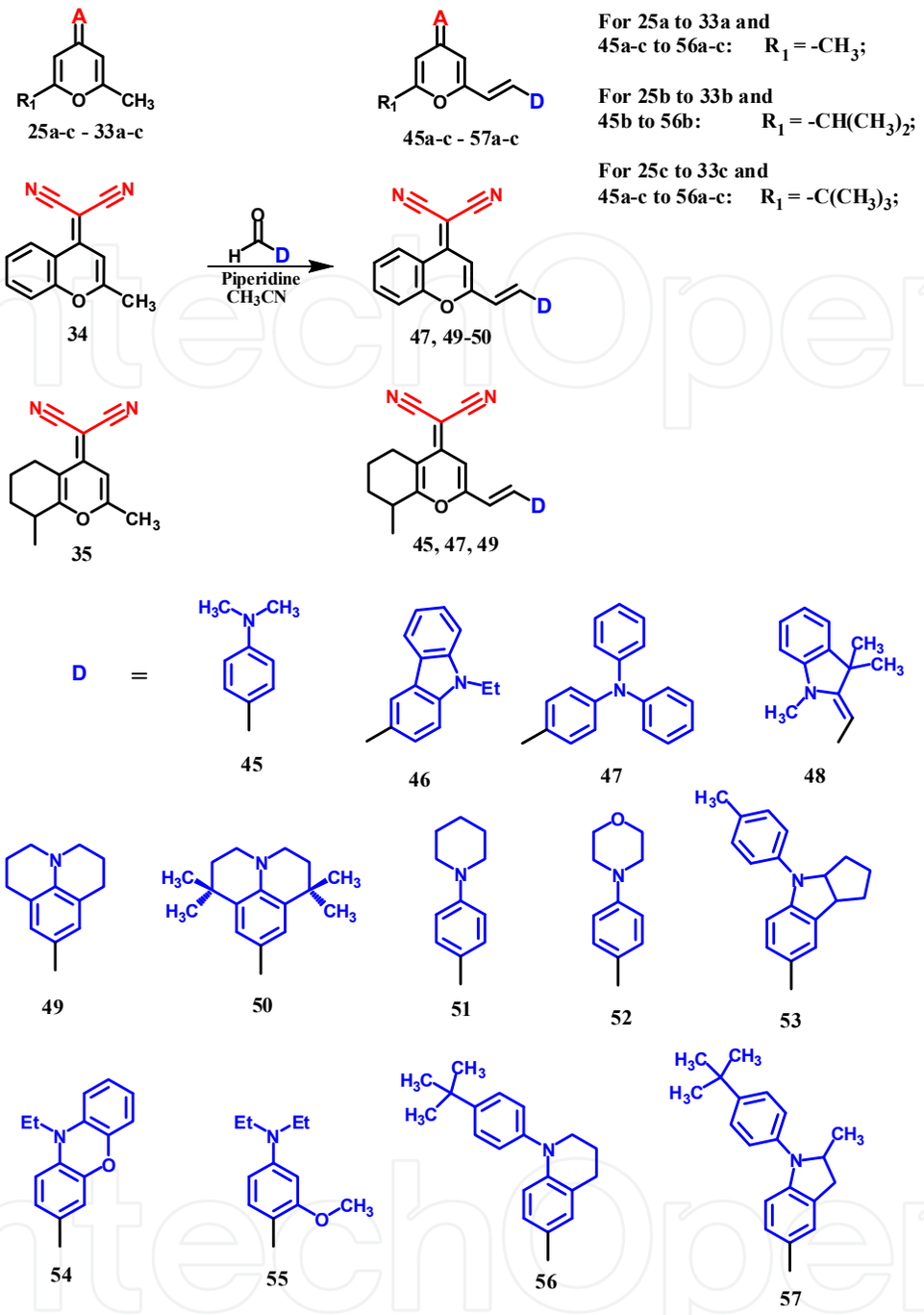

Figure 13. Synthesis of fully functional mono-styryl substituted derivatives of pyranylidene. Electron acceptors are marked in red, electron donors is blue and structure backbone remains in black.

If a pyranylidene backbone with different electron acceptor fragments contains two active methyl groups, then in reaction with a two aldehyde group containing compounds a polymer is formed during the reaction (see Fig.15) [38]. The resulting polymers **70-72** are also reported to be red light-emitting materials.

All derivatives of pyranylidene and isophorene reported so far in this chapter are deposited on the OLED hole transport layer either by thermal evaporation in vacuum or used as dopants in a polymer matrix in limited concentrations.

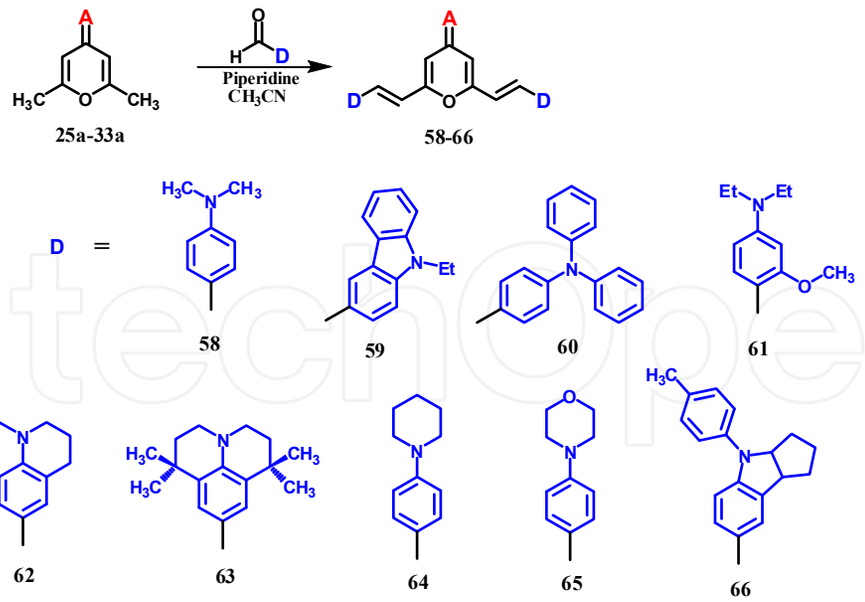

Figure 14. Synthesis of fully functional di-styryl substituted derivatives of pyranylidene. Color significance is the same as for previous figures.

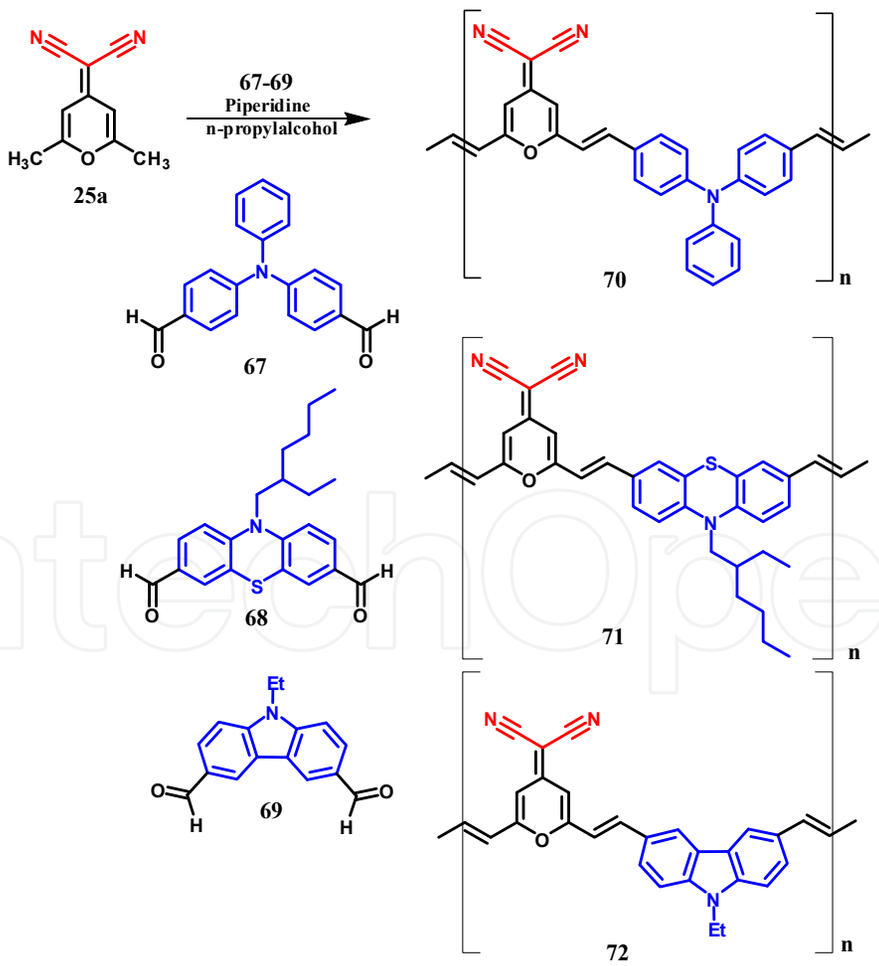

Figure 15. Synthesis of polymeric derivatives of pyranylidene. Color significance is the same as for previous figures.

3. Synthesis and properties of trityloxy group containing glassy derivatives of pyranylidene and isophorene

Our key for obtaining glass forming materials is the synthesis of such electron donor substituent containing aldehyde which would ensure the formation of an amorphous structure of our newly synthesized derivatives of pyranylidene and isophorene. We have synthesized such a compound - 4-(bis(2-(trityloxy)ethyl)amino) benzaldehyde [31-32] **75**, in Fig.16.

3.1. Preparation of molecular glasses

For obtaining a red luminescent glass forming derivative of isophorene, we start with (3,5,5-trimethylcyclohex-2-enone) (compound **29** in Fig.16) as already described in Fig.9. It is subjected to the *Knoevenagel* condensation reaction with malononitrile (**28**). However, 2-(3,5,5-trimethylcyclohex-2-enylidene)malononitrile (**61**) which is formed during the reaction is not isolated because 4-(bis(2-(trityloxy)ethyl)amino) benzaldehyde (**75**) is added to the reaction mixture after 2 hours [31, 37] for further reaction. 2-(3-(4-(Bis(2-(trityloxy)ethyl)amino)styryl)-5,5-dimethylcyclohex-2-enylidene)malononitrile (**IWK)** was obtained in good yield after its separation and purification by liyquid column chromatography as described in [31].

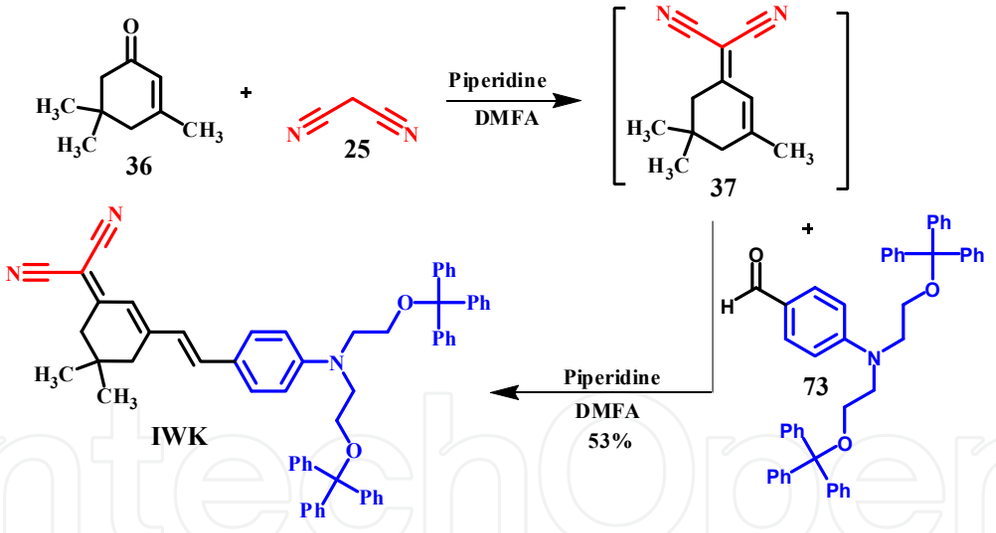

Figure 16. "One pot" synthesis of **IWK.** (See previous figures for explanation of color significance).

For obtaining red luminescent glass forming derivatives of pyranylidene, we use three different electron acceptor fragment containing derivatives of pyranylidene (compounds **25a** in Fig.17). Malononitrile (in compounds **74a and 75a**), indene-1,3-dione (in compounds **74b and 75b**) and barbituric acid (in compounds **74c and 75c**) are used as electron acceptor fragment carrying compounds [32].

In the *Knoevenagel* condensation reaction with compound **25a** and 4-(bis(2-(trityloxy)ethyl)amino) benzaldehyde (**73**) a mixture of mono- (**ZWK-1**, **DWK-1**, **JWK-1**) and bis- (**ZWK-2**, **DWK-2**, **JWK-2**) condensation products is obtained. Their separation is

complicated but nevertheless a large part of each product was separated by liquid column chromatography (silicagel and dichloromethane for **ZWK-1** and **ZWK-2**, dichloromethane: hexane = 4:1 for **DWK-1** and **DWK-2**, dichloromethane: ethyl acetate = 4:1 for **JWK-1** and **JWK-2**). The physical properties of compounds **WK-1**, **WK-2** and **IWK** are described in detail further in this chapter.

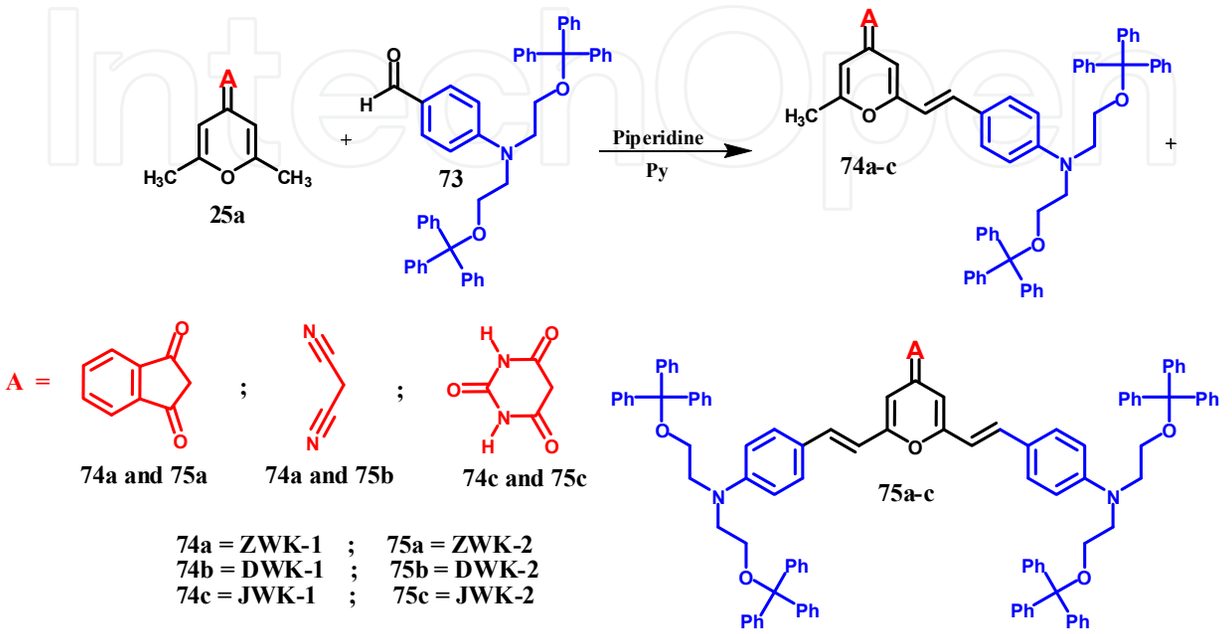

Figure 17. Synthesis of glass forming derivatives of pyranylidene. Py - pyridine. (See previous figures for explanation of color significance). Since compounds **74a-c** and **75a-c** are our obtained red light-emitting materials, we have assigned specific names for each (**ZWK-1**, **ZWK-2**, **DWK-1**, **DWK-2**, **JWK-1** and **JWK-2**) [28-30, 32, 46].

3.2. Thermal properties

The thermogravimetric analysis (TGA) of trityl group containing pyranylidene type compounds is used to measure their thermal decomposition temperatures (T_d). T_d of compounds **WK-1** and **WK-2** are determined in the temperature range from +30°C to +510°C at a heating rate of 10°C/min [32] at the level of 10% weight loss (see Fig.18).

Pyranylidene type compounds with two N,N-ditrityloxyethylamino electron donor fragments (**ZWK-2**, **DWK-2**, **JWK-2**) are slightly more thermally stable than compounds containing only one such fragment, i.e. **ZWK-1**, **DWK-1** or **JWK-1**. The increase in thermal stability of pyranylidene type compounds by adding another electron donor fragment is as high as 10°C from **ZWK-1** to **ZWK-2**, 19°C from **JWK-1** to **JWK-2** and 29°C from **DWK-1** to **DWK-2**. The most thermally stable compound is a two electron donor fragment containing derivative of pyranylidene with malononitrile as electron acceptor in it (**DWK-2**).

Differential scanning calorimetry (DSC) measurements are used to measure the glass transition temperatures (T_g) of the compounds **WK-1** and **WK-2.** Three thermo cycles are performed for the determination of T_g. The first scan was done within the temperature range

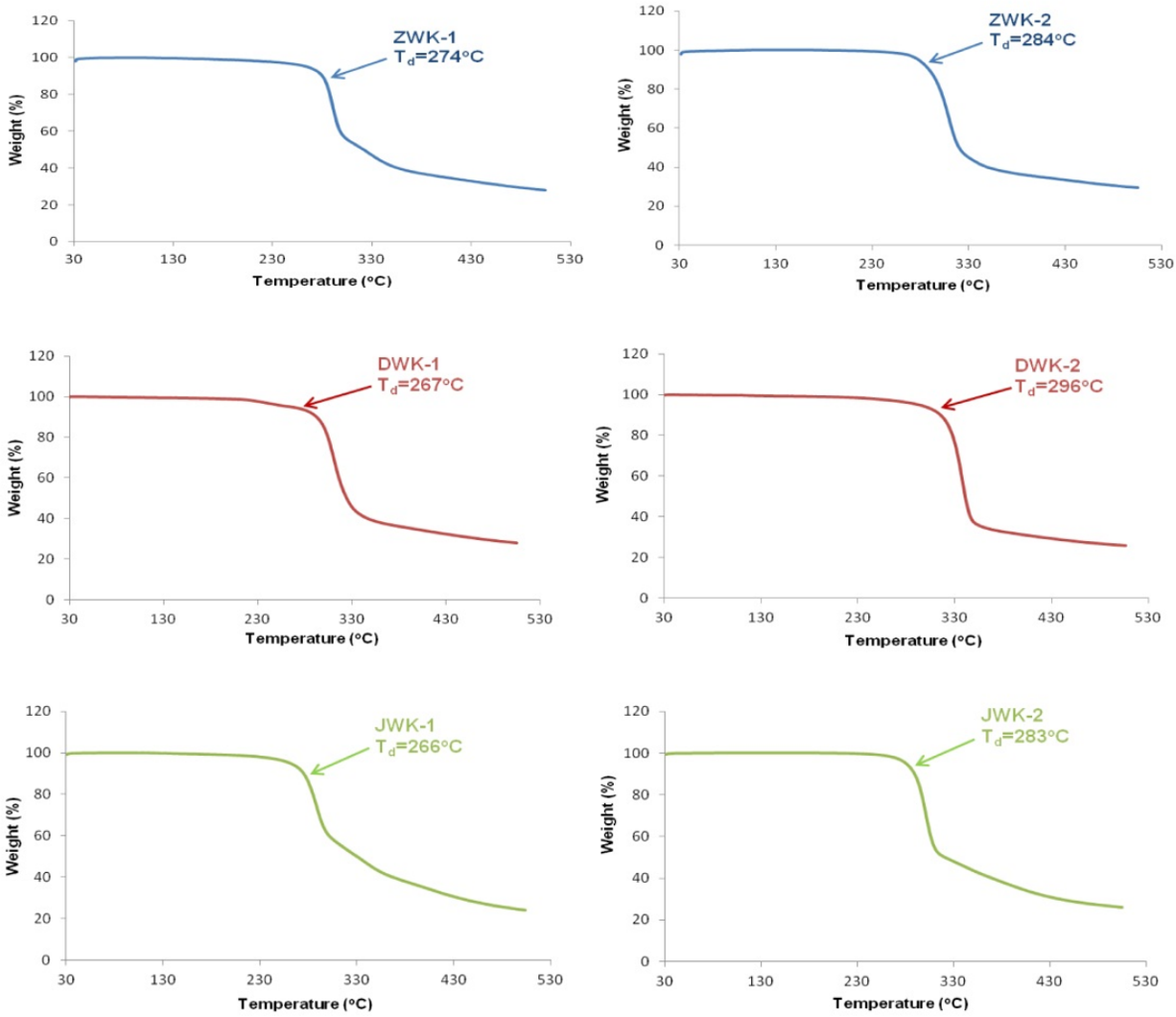

Figure 18. Thermogravimetric analysis of compounds **WK-1** and **WK-2.** A sample of each compound is constantly weighed during heating. At some temperature (T_d) the mass of the sample starts to decrease rapidly - this indicates when the respective compound starts to decompose and is no longer thermally stable.

from +25°C to +250°C at a heating rate of 10°C/min [32]. After the first heating scan samples of the compounds were cooled to 25°C at a rate of 50°C/min and heated for a second time from +25°C to +250°C at a rate of 10°C/min. The T_g value is obtained from the second heating scan (see Fig.19) and for almost all compounds is higher than 100°C. We could not obtain usable DSC curves for **DWK-1**. The compounds with two N,N-ditrityloxyethylamino electron donor fragments have higher T_g compared to those with only one electron donor fragment, which may be attributed to the different numbers of bulky trityloxyethyl groups attached to the two electron donor fragment. In a larger number of bulky groups T_g increases by 8°C from **ZWK-1** to **ZWK-2** and 7°C from **JWK-1** to **JWK-2**. Pyranylidene type compounds with barbituric acid as electron acceptor, e.g. **JWK-1** and **JWK-2** have the highest T_g values compared to **ZWK-1**, **ZWK-2** and **DWK-2**, which may be due to the

additional formation of intermolecular hydrogen bonds by N-H groups of barbituric acid fragments in the molecules.

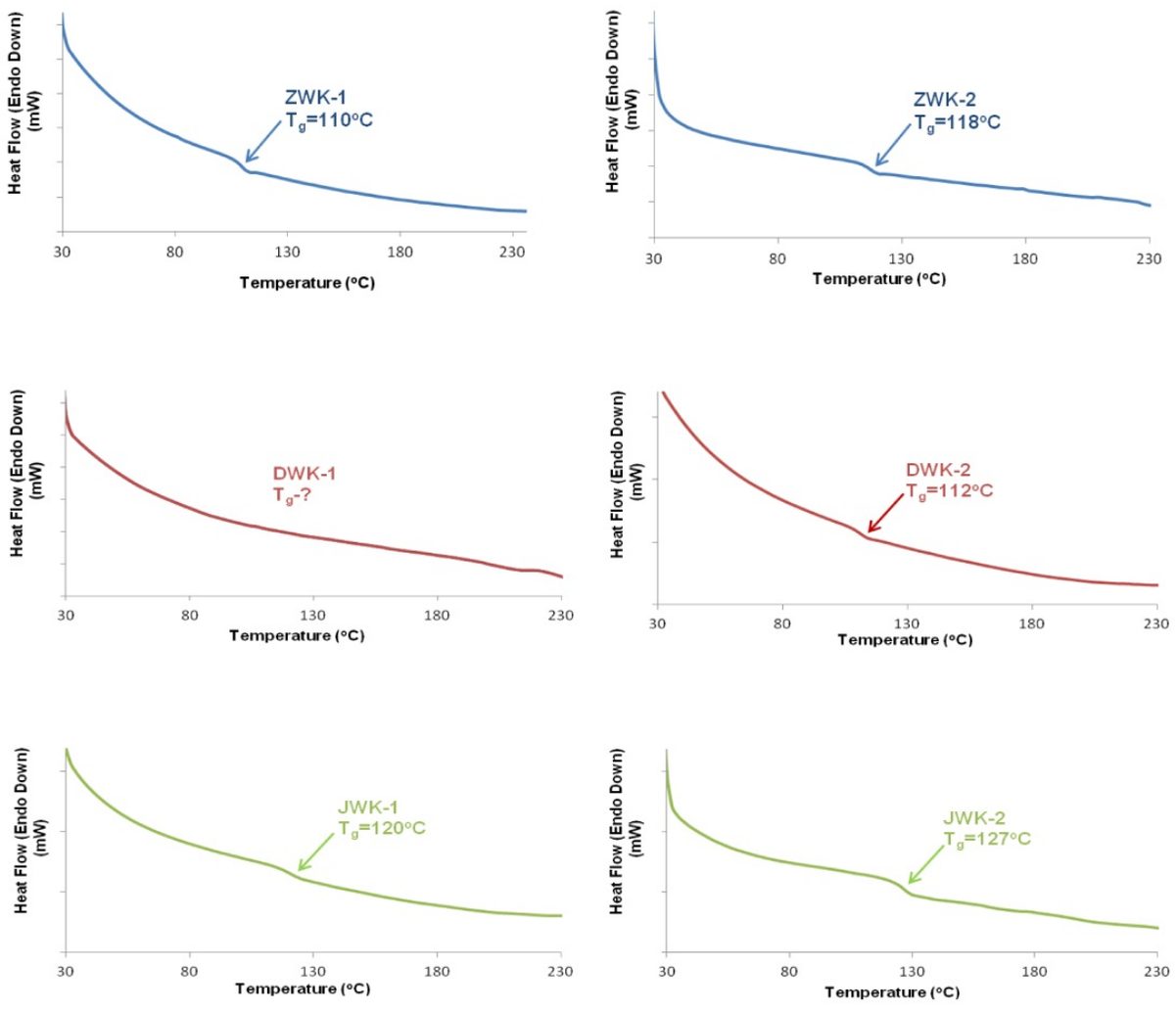

Figure 19. DSC thermogramms of compounds **WK-1** and **WK-2.** Since amorphous compounds have several solid state phase modifications, the glass transition temperature (T_g) indicates when compound solid structure transitions from a more kinetically stable phase (with more free volume) to a more thermodynamically stable phase (with less free volume). During such phase transitions some ammount of heat is absorbed (endothermic process) which appears as a small drop on the DSC curves.

The TGA analysis of **IWK** is conducted as previously described [32]. The thermal decomposition temperature (T_d) of **IWK** is found to be even higher than that of pyranylidene type compounds **WK-1** and **WK-2** (see Fig.20). However its glass transition temperature (T_g) is lower by 18°C to 35°C degrees compared to that of pyranylidene type glasses. Despite the lower thermal stability, the pyranylidene type compounds **WK-1** and **WK-2** have better glass forming properties than the isophorene type compound **IWK**.

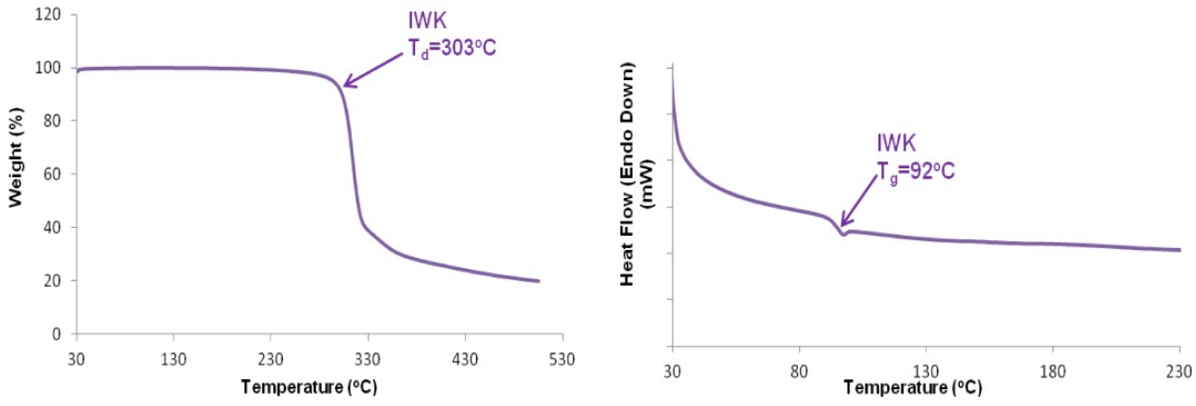

Figure 20. TGA and DSC analysis of **IWK.** (Please see Fig.18 and Fig.19 for a more detailed explanation).

3.3. Glass forming properties

Thin films are deposited on quartz glass by the spin-coating technique. Before the deposition of the layers, the quartz glass substrates are cleaned in dichloromethane. The solutions are spin-coated onto the substrates for 40 s at 400 rpm and acceleration 200 rpm/s.

In all cases, pure films obtained from two electron donor fragment containing pyranylidene compounds (**ZWK-2**, **DWK-2** and **JWK-2**) have an almost pure smooth and amorphous surface, but pyranylidene compounds with one electron donor fragment (**ZWK-1**, **DWK-1** and **JWK-1**) show several crystalline state areas (see Fig.21). Both glasses containing barbituric acid as an electron acceptor fragment (**JWK-1** and **JWK-2**) show the least amount of small crystal formations on their pure film surface. The higher stability of their amorphous state could be explained by an enchancement of N-H group hydrogen bonds in the molecules. Pure films obtained from malononitrile electron acceptor fragment containing compounds (**DWK-1** and **DWK-2**) contain small crystal dots, especially **DWK-1**. This could be due to small steric dimensions of malononitrile group, which allows more **DWK-1** molecules to be concentrated in the same volume to allow closer interaction with other molecules enabling higher possibility to form agreggates and crystallites.

Information obtained from the surfaces of the pure films is consistent with the measured glass transition temperatures (T_g). Glasses having higher T_g values are found to have less crystalline dots on their pure film surface. As we were unable to determinate T_g for **DWK-1**, according to above mentioned trend its glass transition temperature is expected to be below 110°C.

Thin film containing only pyranylidene type compound **WK-1** and **WK-2** are amourphous despite of small crystalline dots in it. Till now only way to prepare amourphse films which contain pyranyliden derivatives was doping them in glass forming compound. In that case maximum doping concentration was considered to be 2wt% due to self crystallization [11-12]. However, incorporation of bulky trityloxy groups in their molecules or using glasses **WK-1** and **WK-2** could increase this concentration limit more then 10 times.

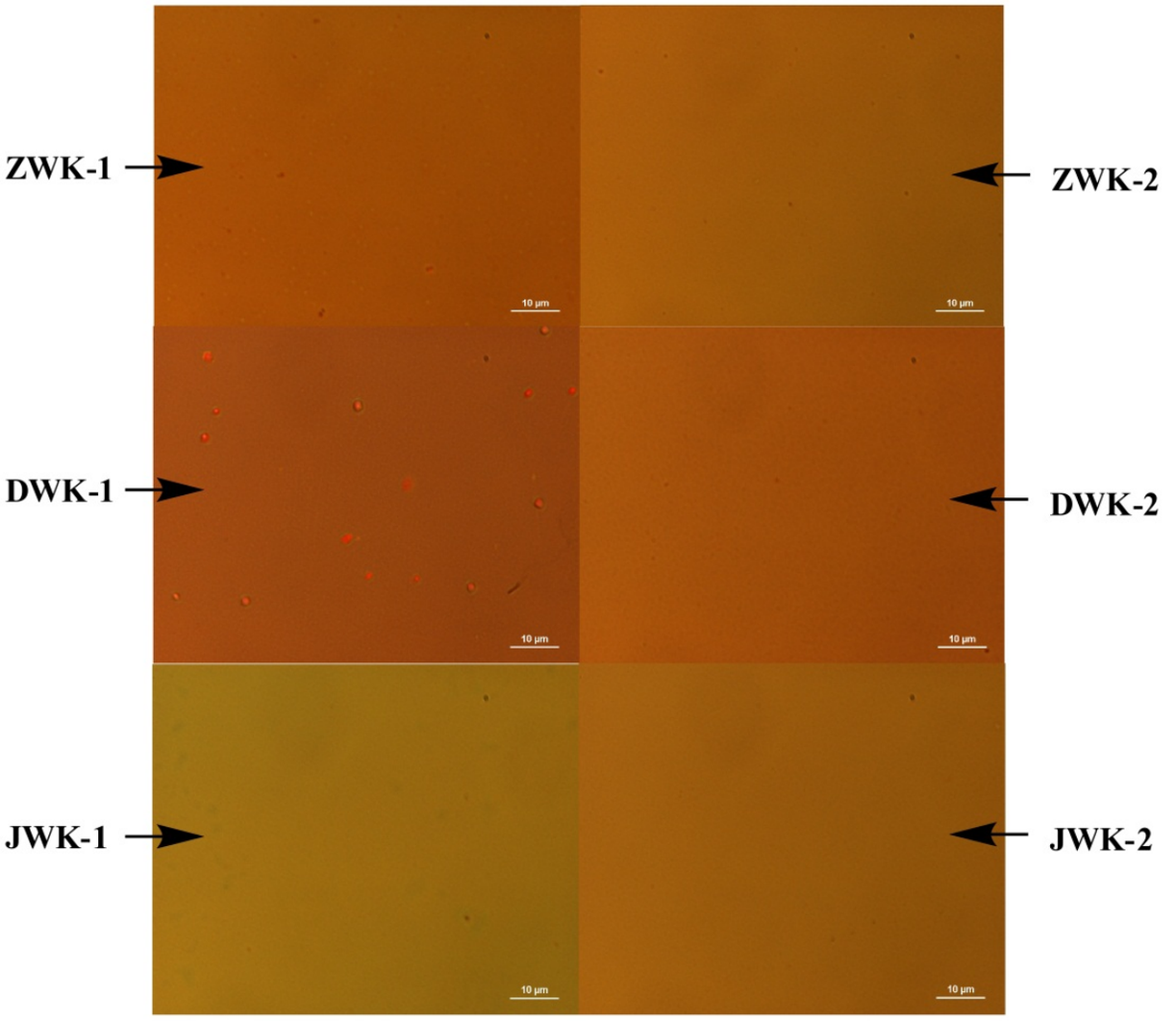

Figure 21. Optical mircroscope images of the pure films of the compound **WK-1** and **WK-2**. Dots on the pure film surface represent compound crystalline state while the remaining smooth area shows amorphous solid state.

3.4. Absorption and luminescence properties

The absorption and fluorescence spectra of the synthesized compounds in diluted dichloromethane solution and pure films are shown in Figs. 22 and 23.

A **DWK-1** molecule, whose backbone consists of the laser dye 4-(dicyanomethylene)-2-methyl-6-[p-(dimethylamino)styryl]-4H-pyran (**DCM**), in dichloromethane solution has its absorption maximum at 472 nm, which is 8 nm red shifted with respect to the pure **DCM** molecule in the same solution [9]. It shows that the bulky trityloxyethyl group has only a small influence on the energy structure of the molecule. The peaks of the absorption spectra in solution of the molecules with indene-1,3-dione (**ZWK-1**) and barbituric acid (**JWK-1**) electron acceptor substituents in the backbone are red-shifted by approximately 40 nm compared to **DWK-1**. A stronger electron acceptor group gives larger red shifts.

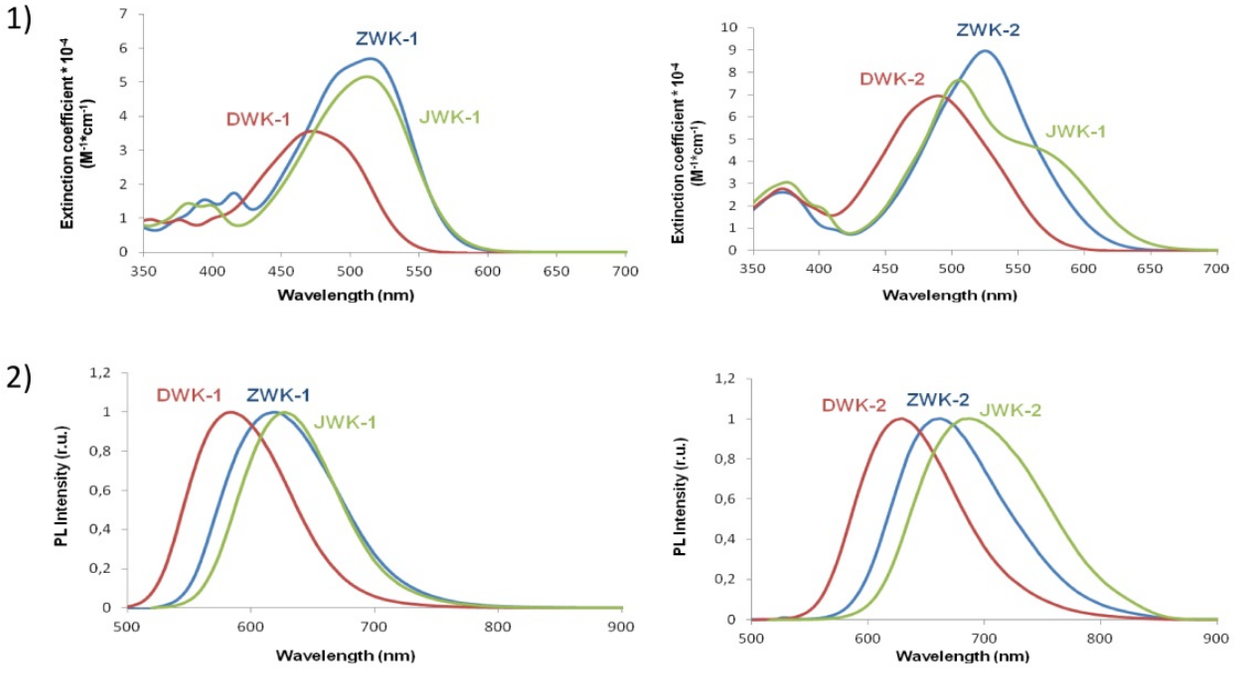

Figure 22. 1) Absorption and 2) Photoluminescence spectra of compounds **WK-1** and **WK-2** in dichloromethane solution

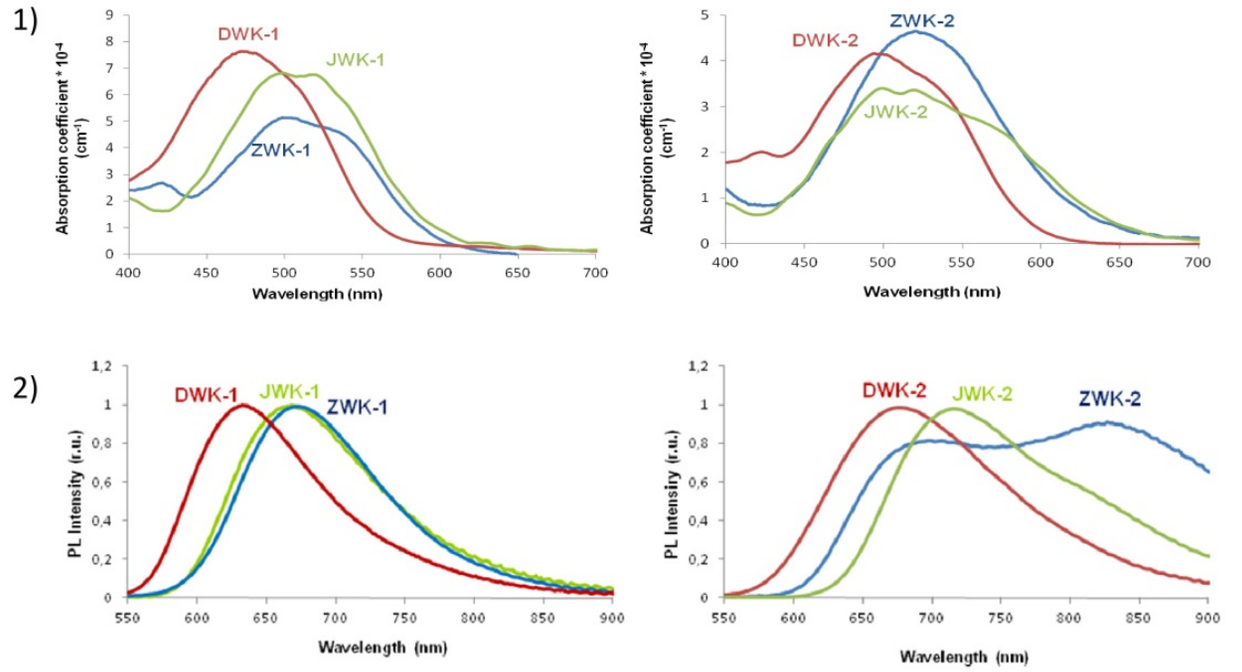

Figure 23. 1) Absorption and 2) Photoluminescence spectra of compounds **WK-1** and **WK-2** in thin solid films

The photoluminescence (PL) spectrum of the **DWK-1** solution was found to be Stokes shifted by about 115 nm (peak position at 587 nm) with respect to the absorption spectra (see Fig.22). The PL spectra of **JWK-1** and **ZWK-1** molecules exhibited similar shapes, with their

maxima red-shifted to 635 and 627 nm, respectively. The photoluminescence spectra are unstructured and strongly Stokes shifted in accordance with intramolecular charge-transfer nature of the excited states [39]. For compounds containing two 4-((N,N-ditrityloxyethyl) amino)styryl electron donor fragments the absorption and luminescence spectra of the solution are observed to be red-shifted and have larger extinction coefficients, which is due to the larger absorption cross section of these molecules. The peaks of the absorption spectra of **DWK-2** and **ZWK-2** are red shifted by 17 and 11 nm, respectively, compared to molecules with a single electron donor fragment. A similar red shift has been reported for the molecule with two electron donor fragments **bis-DCM** compared with **DCM** molecules with a single electron donor fragment [40]. It is observed that molecules with two electron donor fragments have a larger conjugation length. A second reason could be simultaneously functioning two donor groups which give stronger electron donor properties. The shape of the absorption spectrum of **JWK-2** is found to be different from that of **JWK-1** and the oscillator strength of the absorption band of **JWK-2** at about 502 nm becomes more intense (see Fig.22(1)).

The fluorescence spectra of molecules with two electron donor fragments are broader and further Stokes shifted than molecules with only one electron donor fragment. This may be attributed to the different conjugation lengths as indicated by the absorption spectra. The peak positions of **DWK-2**, **ZWK-2** and **JWK-2** are observed at 640, 678 and 701 nm, respectively. The red shift of the absorption spectra of solutions increases corresponding sequentially to **ZWK**, **JWK** and **DWK**, as stronger electron acceptor fragments induce larger red shifts. This could be explained by their electron withdrawing properties, which differ among our investigated electron acceptor fragments. The shift of luminescence spectra did not maintain the same sequence due to the larger Stokes shift for the **JWK** molecules.

The absorption spectra of thin solid films of the molecules with one electron donor fragments are practically unchanged with respect to the solutions spectra. They are slightly broader with small red-shift indicating a weak excitonic interaction in the solid state, which is typical for glass-forming amorphous materials. For the molecules with two electron donor fragments **ZWK** and **DWK** the absorption spectra are found to shift by 21 nm and 22 nm, respectively. The peak positions of the absorption spectra for **JWK** molecules remain unchanged by the incorporation of a second electron donor fragment. However, the fluorescence spectra of all films are red-shifted in comparison with those of solution.

For molecules with one electron donor fragment, the shape of the fluorescence spectra of thin films is very similar to that in solution, which confirms that for these compounds the excited states in the aggregates in the solid state are not very different from those in molecules. However, the derivatives with two electron donor fragments exhibit an additional band at longer wavelengths in thin films, which becomes more intense going from weaker to stronger electron acceptor fragments in the studied molecules. In the case of **ZWK-2** in thin films the additional band even becomes dominant.

In the case of **IWK**, the absorption and luminescence spectra of thin solid films are also found to be practically unchanged compared to its solutions spectra as shown in Fig.24.

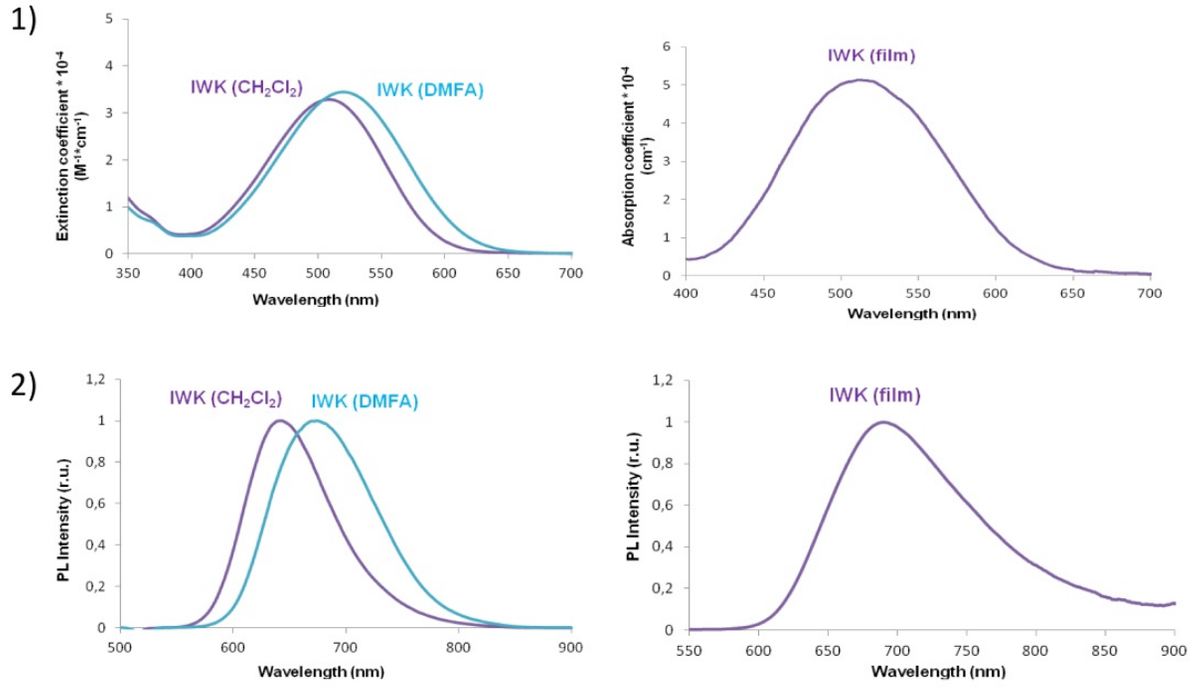

Figure 24. 1) Absorption and 2) Emission of **IWK** in solutions and thin solid film

The same relation is observed for **IWK** emission properties in solution as well as in thin films. However, in solid state its emission is very weak compared to pyranylidene type compounds, which may limit the usefulness of **IWK** in OLED applications.

3.5. Photoluminescence quantum yields

Photoluminescence quantum yield (PLQY) of the investigated compounds in solution and in thin films is measured by using an integrating sphere (Sphere Optics) coupled to a CCD spectrometer [41]. PLQY thus measured for all compounds are summarised in Table 3. Compounds with more polar groups attached exhibit PLQY up to 0.54 in dilute solutions, which is slightly higher than for **DCM** dye in similar surroundings [42, 43]. PLQY depends slightly on the acceptor group as can be seen from Table 3. That means that compounds with a stronger electron acceptor group have higher PLQY. **JWK** and **ZWK** molecules with two electron donor groups have lower PLQY in comparison with one electron donor group. However, the opposite is observed with **DWK** compounds, as molecules with two electron donor groups exhibit larger PLQY. This may be due to the shielding of the acceptor group by bulky trityloxyethyl groups. PLQY of pure films is found to be more than one order of magnitude lower than that in solution. This reduction is particularly strong in the case of molecules with two donor groups. PLQY values of these compounds correlate with the intensity of the long wavelength fluorescence band, as PLQY is lower in materials with a stronger low energy fluorescence band. Molecular distortions taking place during formation of solid films are probably responsible for both of these effects. Compound molecules with

two bulky acceptor groups are probably strongly distorted in solid films, so that molecular chains connecting acceptor and donor moieties are twisted. Such twisting usually leads to a red-shift in the molecular fluorescence and to fast non-radiative relaxation [44]. The twisted molecules form energy traps in solid films, which may be populated during the excitation diffusion. Therefore, even a small fraction of distorted molecules may significantly affect the fluorescence spectrum and PLQY. We were unable to measure PLQY in **IWK** pure thin solid films. Moreover, it also shows the lowest value in solution and therefore cannot be used as a light-emitting material.

	Solution	Thin film
DWK-1	0.32	0.026
DWK-2	0.43	0.009
JWK-1	0.47	0.011
JWK-2	0.32	0.007
ZWK-1	0.54	0.01
ZWK-2	0.4	0.003
IWK	0.098	-

Table 3. Photoluminescence quantum yield of investigated molecules in dichlormethane solutions and pure thin films.

It is worth mentioning that **DCM** molecules do not show any photoluminescence from pure films due to the small distance between molecules which results in high molecular interaction. Therefore, host-guest films of transparent polymethylmethacrylat (**PMMA**) polymer with varying dye doping were prepared in order to observe the impact of concentration on photoluminescence quenching. The dependence of PLQY on concentration of **DWK-1** and **DWK-2** molecules is shown in Fig.25.

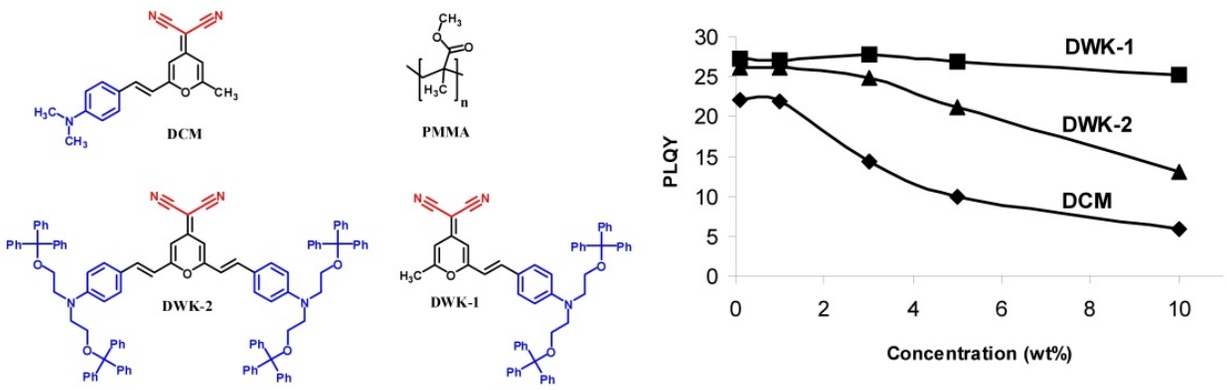

Figure 25. The dependence of PLQY on concentration of **DWK-1**, **DWK-2** and **DCM** dyes in **PMMA** matrix.

For comparison the PLQY of **DCM** in **PMMA** are also included in Fig.25. **PMMA** films doped with **DWK-1** and **DWK-2** at low concentration (<1 wt%) exhibit somewhat lower PLQY as compared to that obtained in solution (See Fig.24 and Table 3). This discrepancy may be attributed to the sensitivity of molecules to the polarity of the surrounding media.

At higher concentrations (>3 wt%) the **DWK-1** molecule shows negligible photoluminescence quenching dependence on concentration. On the other hand molecules with two donor groups exhibit pronounced quenching. Fluorescence efficiency of the polymer film doped with 10 wt% of **DWK-2** molecules decreases 2-times compared to that of films doped with 10 wt% **DWK-1** molecules. The reason for the lower PLQY could be the same as for different PLQY of the pure films. The laser dye **DCM** dispersed in the polymer matrix at high concentration shows a remarkable fluorescence quenching. For example, at a 10 wt% concentration of **DCM** molecules, up to a 4-time decrease of quantum yield is observed in comparison with the same concentration of **DWK-1** molecules. Thus, incorporation of bulky trityloxyethyl groups prevents the formation of aggregates of the dye molecules and remarkably reduces the fluorescence quenching dependence on concentration, enabling the use of higher doping levels in emissive layers.

3.6. Amplified spontaneous emission properties

DCM molecule is a well known laser dye. In a previous work light amplification was demonstrated in **DCM:Alq$_3$** (see Fig.25 and Fig.26) thin films [45].

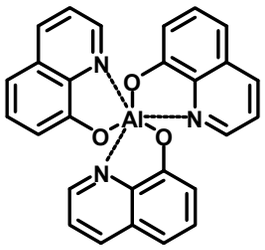

Alq3

Figure 26. Tris(8-hydroxyquinolinato)aluminium (**Alq3**) is a well known light-emitting material.

In order to test the light amplification prospects of our synthesized compounds, we prepared pure thin films of all the compounds on a quartz substrate and measured their amplified spontaneous emission (ASE). Such emission was observed only for four of six compounds, **DWK-1**, **DWK-2**, **JWK-1** and **ZWK-1,** as shown in Fig.27 [46].

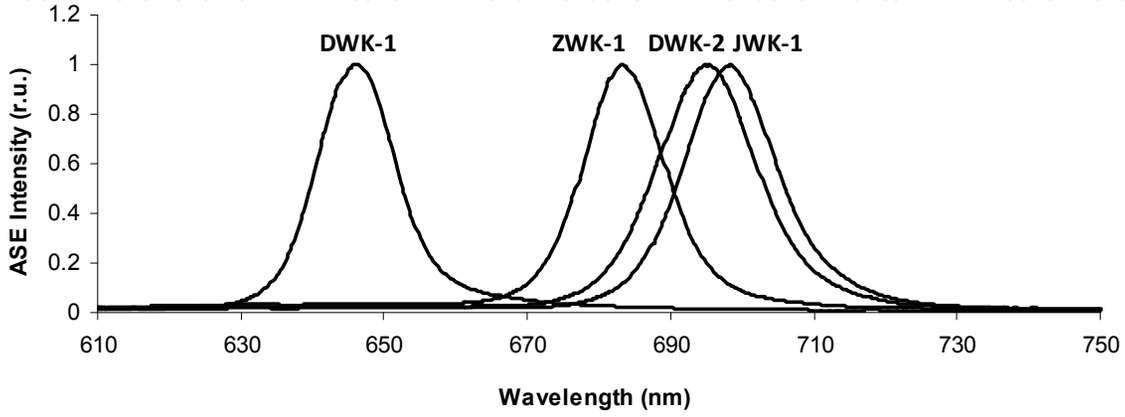

Figure 27. ASE spectrum in pure films of compounds **ZWK-1**, **DWK-1**, **DWK-2** and **JWK-1**

From the other two samples of **JWK-2** and **ZWK-2** no ASE signal has been observed. The peak positions of ASE are red shifted as compared to the fluorescence band maxima (see Fig.27 and Fig.22). The red shift values were found to be 14, 18, 10 and 31 nm for **DWK-1**, **DWK-2**, **JWK-1** and **ZWK-1,** respectively. Variations in the peak intensity of ASE spectra as a function of the pump beam pulse energy are shown in Fig.28, from which ASE threshold values are estimated to be 90±10, 330±20, 95±10, 225±20 μJ/cm² for **DWK-1**, **DWK-2**, **JWK-1** and **ZWK-1**, respectively. These values are larger in comparison with the threshold values (of the order of micro joules per square centimeter) reported for some other materials [46, 47].

However, a direct comparison is difficult because the ASE threshold, in addition to material properties, depends also on the sample and excitation geometries, film thickness, optical quality and excitation pulse duration.

Nevertheless it has not been observe ASE in pure **DCM** films, but we have measured it in **DWK-1** which is the same **DCM** with additional trityloxyethyl group. It should also be noted that some sample degradation has been observed at the highest excitation intensities; however no noticeable degradation is observed when excitation intensity is 1.5 - 2 times exceeding the ASE threshold.

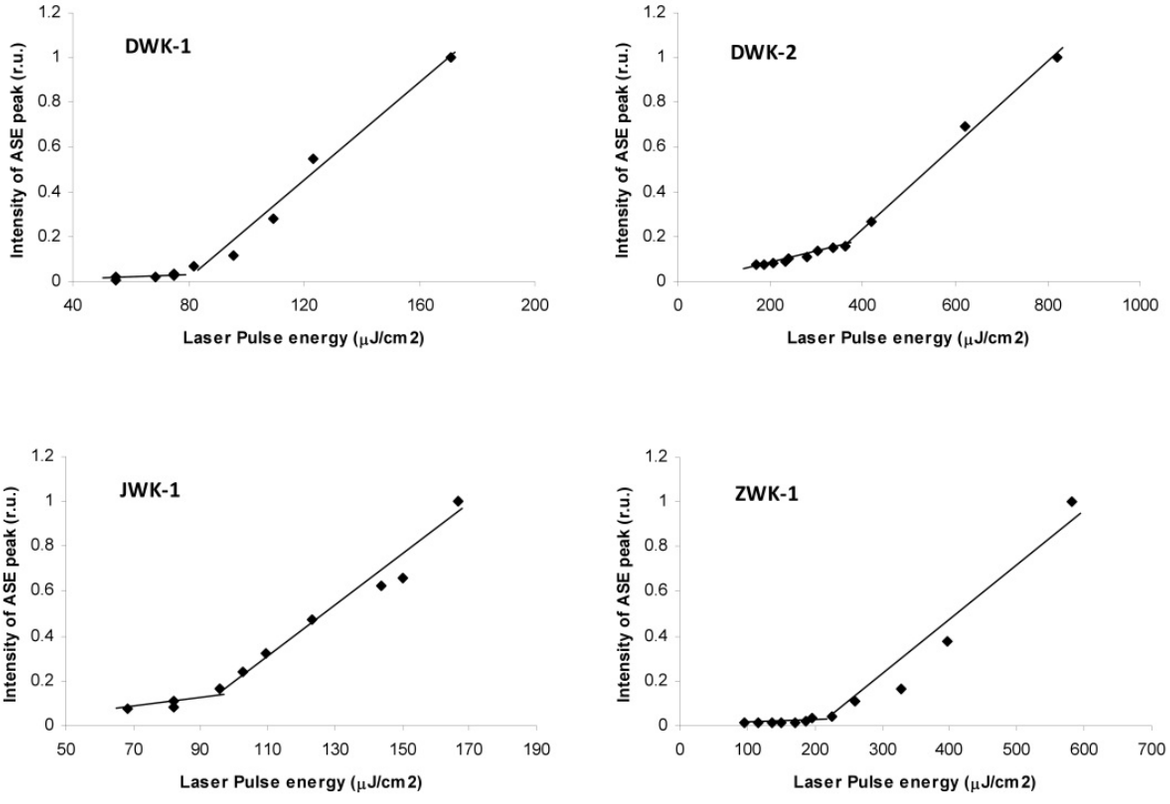

Figure 28. ASE intensity as a function of irradiation pulse energy in **DWK-1**, **DWK-2**, **JWK-1**, **ZWK-1** compounds in thin solid film. Lines are guides for the eye.

ASE develops in the spectral position where the light amplification coefficient has the maximal value. The amplification coefficient may be described as:

$$a(\lambda) = n^* [(\sigma_{em}(\lambda) - \sigma^*(\lambda)] - (N - n^*)\sigma_0(\lambda) \quad (1)$$

where n^* is the density of excited molecules, N is the total density of molecules, $\sigma_0(\lambda)$,$\sigma_{em}(\lambda)$and $\sigma^*(\lambda)$ are cross-sections of the ground state absorption, stimulated emission and excited state absorption, respectively. As it can be seen from Eq. (1) even weak ground state absorption may strongly reduce the amplification coefficient or make it negative. This is because only a small fraction of molecules is usually excited even under high intensity excitation conditions, i.e., N>>n*. Thus, the absorption band tails, which overlap with fluorescence band, are evidently responsible for the red shifts in ASE spectra in comparison with the maxima of the fluorescence. Note, that the light propagation length is limited by the film thickness in the absorption measurements, while ASE emission can propagate a much longer way along the film.

3.7. Photoelectrical properties and energy structure of glassy thin films

Information about the location of energy levels enables one to determine the best sample structure for electroluminescence measurements. To characterize the energy gap in organic solids several methods are applied. In organic crystals as well as amorphous solids charge carriers do not emerge as "bare" quasi-free electrons and holes but as a polaron type quasi-particle, dressed "in electronic and vibronic polarization clouds" [48, 49]. Electronically relaxed charges may be formed far enough from each other which give rise to a wider optical band gap E_G^{Opt} [49, 50]. The optical energy gap E_G^{Opt} may be obtained from the low energy threshold of the absorption spectra of organic thin films. The vibrationally and electronically relaxed charge carrier states contribute to the adiabatic energy gap E_G^{Ad}. It could be attributed to the threshold energy of photoconductivity E_{th} which can be estimated from the spectrum of the quantum efficiency of photoconductivity $\beta(h\upsilon)$ [49]:

$$\beta(h\nu, U) = \frac{j_{ph}(h\nu, U)}{k(h\nu)I(h\nu)g(h\nu)} \quad (2)$$

where j_{ph} is the density of photocurrent at a given photon energy hν and applied voltage U, I(hν) is the intensity of light (photons/cm^{2}s), k(hν) is the transmittance of the semitransparent electrode and g(hν) is the coefficient which characterizes the absorbed light in the organic layer.

E_{th} can be determined from a sample where the organic compound is sandwiched between two semitransparent electrodes, which in our case are ITO and thermally evaporated aluminum. The sample is irradiated through the electrodes and current changes are measured as shown in Fig.29(1). Efficiency of photoconductivity at different light energy is calculated using Eq. (2) and is plotted as a function of the photon energy in Fig.29(2). The sample is illuminated from both aluminum and ITO side when positive and negative voltage is applied to them. E_{th} is determined by plotting $\beta^{2/5}$ as a function of the photon energy. The intersections of tangents at low photon energy on the curve of $\beta^{2/5}$ plotted as a function of the photon energy and photon energy axis gives E_{th} as shown in Fig.29(3).

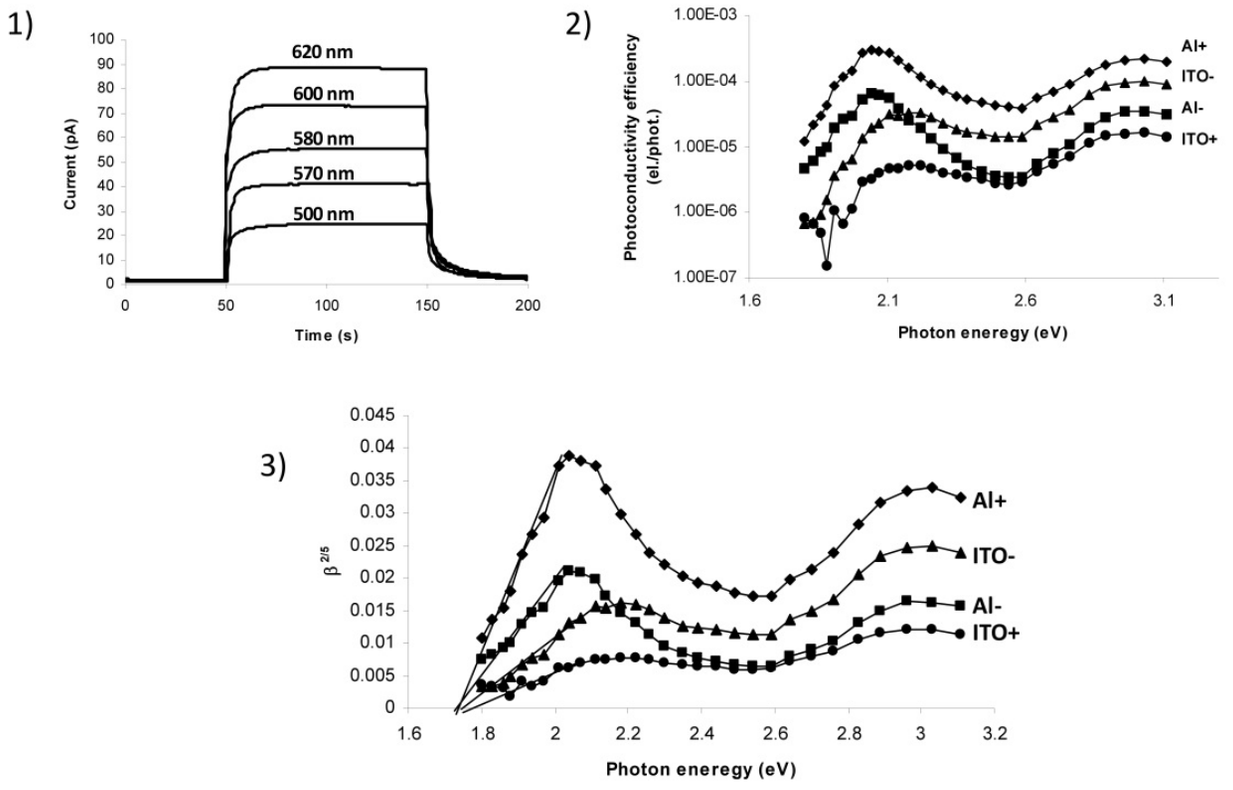

Figure 29. 1) Photocurrent at different wavelength for **JWK-2** compound ,2) Dependency of photoconductivity efficiency on photon energy for **JWK-2** compound,3) Determination of E^{th} from photoconductivity efficiency spectral dependence.

Optical band gap E_G^{Opt}, photoconductivity threshold value E_{th} and reduction-oxidation potential U_{redox}, determined from cyclic voltamperogramme, for investigated compounds are presented in Table 4.

	E_G^{Opt} (eV)	E_{th} (eV)	U_{redox} (V)
DWK-1	2.20	1.92	2.35
DWK-2	2.10	-	1.99
JWK-1	2.08	1.78	2.01
JWK-2	1.88	1.62	1.90
ZWK-1	2.08	1.78	2.04
ZWK-2	1.96	1.68	2.00

Table 4. Optical band gap E_G^{Opt}, photoconductivity threshold value E_{th} and red-ox potential U_{redox} for the compunds **DWK-1**, **DWK-2**, **JWK-1**, **JWK-2**, **ZWK-1**, **ZWK-2**.

According to Table 4, the redox potential of **DWK**, **JWK** and **ZWK** is higher for compounds with one electron donor group compared to compounds with two electron donor groups (see Fig.17). The same relation is found for optical band gap as well.

The photoconductivity threshold value cannot be obtained for **DWK-2** thin films due to the low value of photocurrent. For other compounds we obtain an excellent linear correlation

between optical band gaps and photoconductivity threshold values with correlation coefficient 0.993. The slope of this linear relation is found to be 1 and intercept 0.28 as shown in Fig.31

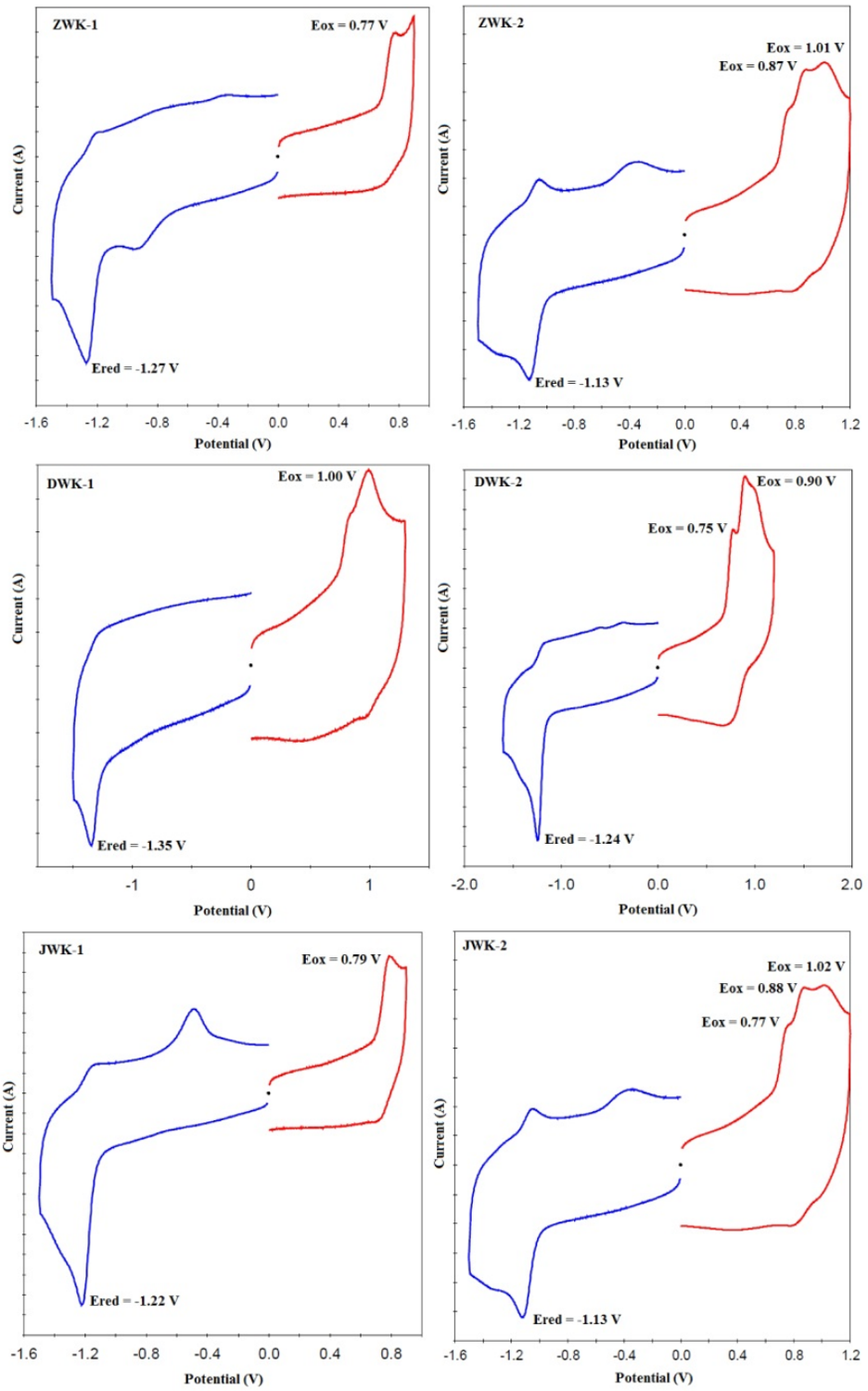

Figure 30. Cyclic voltamperogramme curves of compounds **WK-1** and **WK-2**. Posistive values are oxidation potential and negative values reduction potential.

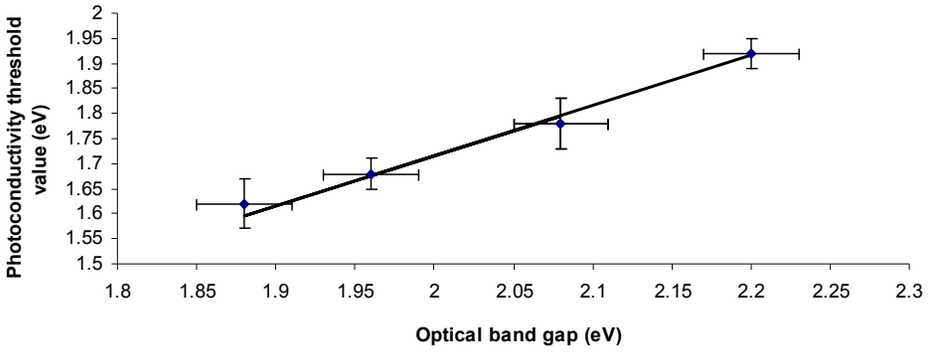

Figure 31. Linear correlation between optical band gap and photoconductivity threshold value. Line is the best fit with slope coefficient one.

The energy of the photoconductivity threshold is defined as the difference between the conduction levels of holes and electrons [51]. The value of the intercept implies that the optical band gap is 0.28 eV larger than the difference between the conduction levels of holes and electrons. It shows a constant energy difference between optical band gap and adiabatic gap despite the various molecule structures.

3.8. Electrical properties

Electrical properties of **WK-1** and **WK-2** compounds are investigated in the regime of space charge limited current (SCLC) [52-54]. Similar sandwich type samples as used for photoelectrical measurements are prepared for this study as well. The thickness of the organic thin film is at least 500 nm.

The current-voltage characteristics of compounds **ZWK-1**, **ZWK-2**, **JWK-1**, **JWK-2** and **DWK-2** in thin solid films are shown in Fig.32.

The current-voltage characteristic of **DWK-1** films could not be measured due to unstable current. This may be due to formation of small crystallites (see Fig.21) around 1 μm in size. Such aggregates are found throughout the sample and induce instability in the current. In all other cases the current-voltage characteristics have similar shapes with three regions. In the first region, 0-2 volts, the current is found to depend linearly on voltage. In the second range, 2 to 50 volts the current increases superlinearly with voltage, following Child's law. In the third region, > 50 V, the current depends on voltage to the power of at least ten, which may be attributable to charge trapping in the local trap states. More details of this aspect will be discussed further below.

Usually the work function of ITO should be near the ionisation energy level of the organic compound while that of aluminium (Al) should be around the middle of the energy gap. This provides efficient hole injection from ITO and electron injection from aluminium when a positive voltage is applied to ITO. Holes may also be injected from the aluminium when positive voltage applied to it. Electron injection may be more difficult in the second case due to the large difference between the ITO work function and electron affinity potential of the

organic compound. This is confirmed by the current voltage characteristics shown in Fig.32. A similar current is observed at the lower voltage where only holes are injected either from ITO or aluminium when biased with a positive voltage. At higher voltage current is higher when ITO is positive in comparison with positive aluminium.

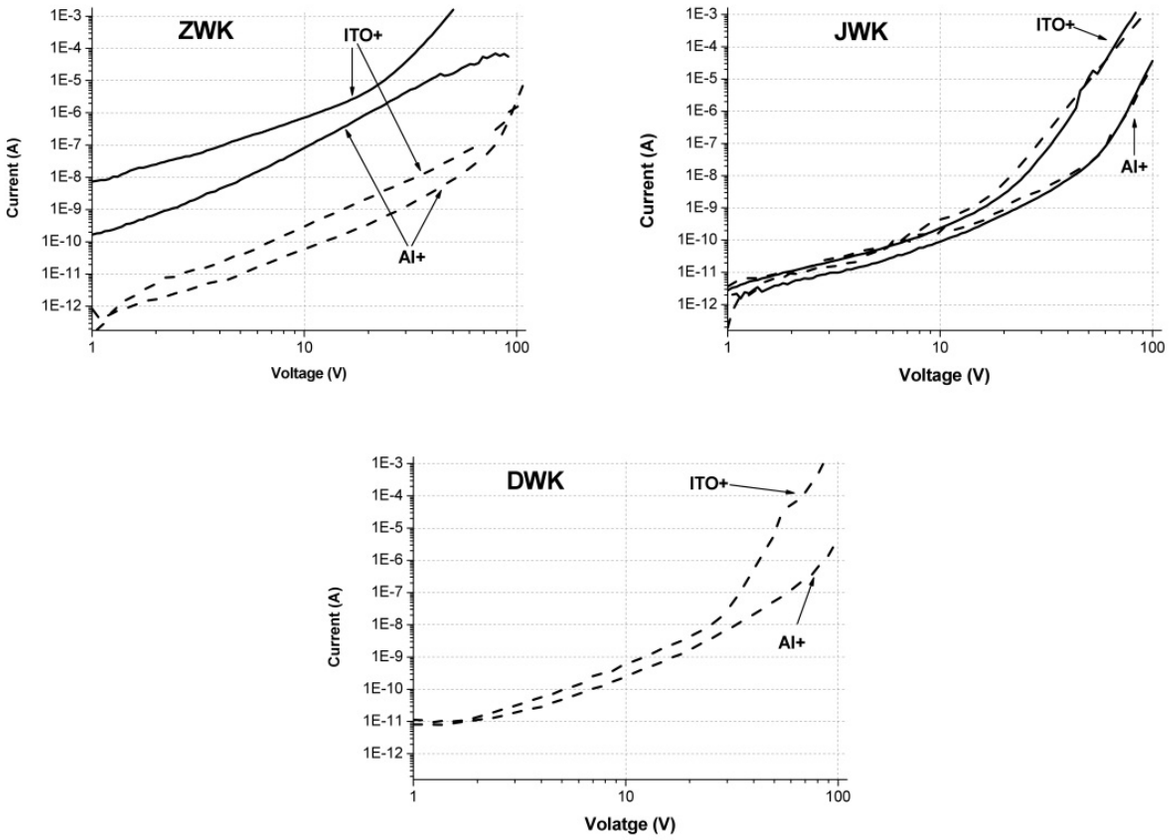

Figure 32. Current-voltage characteristics of pure thin films of **ZWK**, **JWK**, **DWK** compounds. Solid line – compounds with one electron donor group, dashed line - compounds with two electron donor group.

The temperature modulated space charge limit current (TM SCLC) method is used to analyse the charge carrier local trapping states in solid films [55]. The condition for using this method (TM SCLC) is monopolar injection, which is achieved in our case when a positive voltage is applied to the aluminium electrode. The measured activation energy is plotted as a function of the applied voltage for the investigated compounds as shown in Fig.33.

No charge carrier local trap states are found in films of compounds with one electron donor group due to only one plateau which reaches zero. All compounds with two electron donor groups are found to have charge carrier trap states. The additional plateau of activation energy, which can be clearly seen from Fig.33 means that the thin films contain local trap states. The hole shallow trap depths are found to be 0.1, 0.24 and 0.3 eV in **ZWK-2 JWK-2** and **DWK-2,** respectively. Such trap states decrease the efficiency of electroluminescence and should be avoided in fabricating high efficiency light emitting diodes. The activation

energy increases at lower voltage for compounds **JWK-1**, **JWK-2** and **DWK-2**. This is indicative of a contact problem where the electrode – organic interface also works as additional charge carrier traps.

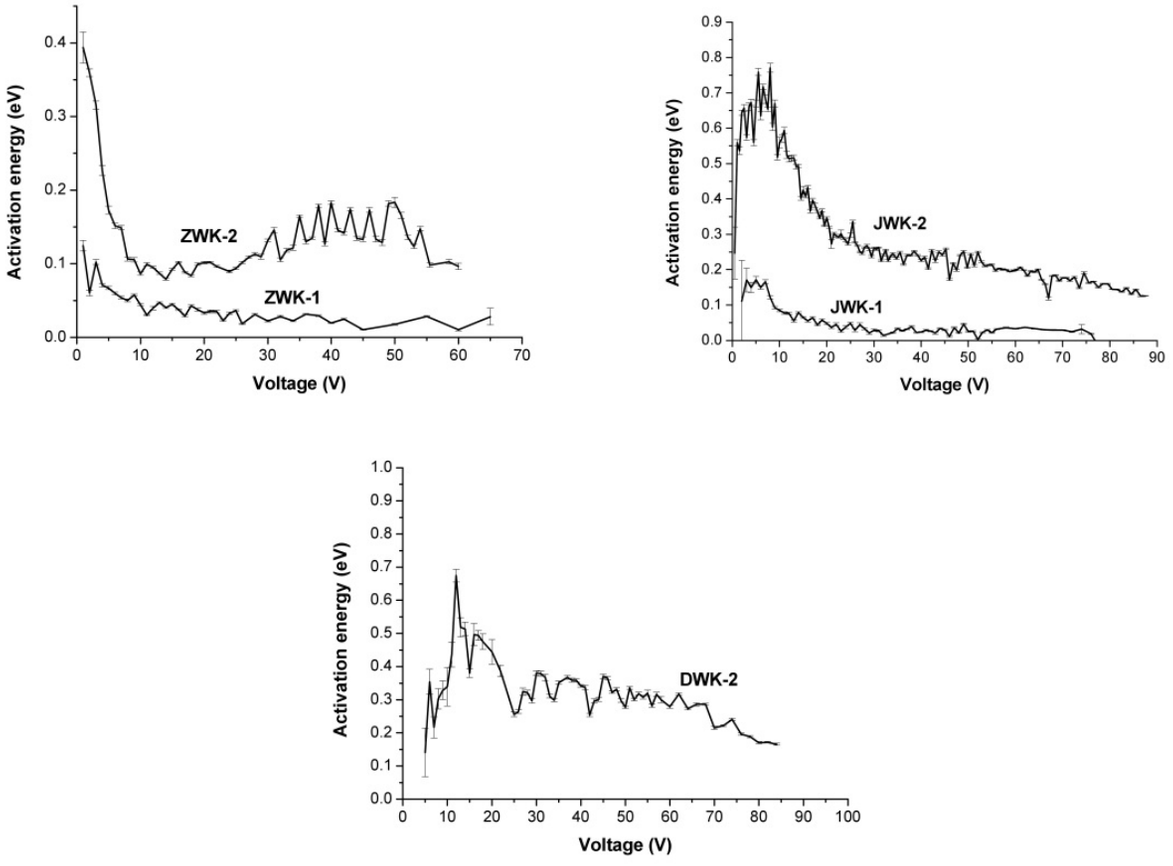

Figure 33. Activation energy dependence on applied voltage of the investigated compounds in solid films. Positive voltage was applied to aluminium electrode.

3.9. Electroluminescence of ZWK-1 and ZWK-2

A multilayer structure is used for electroluminescence (EL) measurements. Polyethylenedioxythiophenne:polystyrenesulfonate (PEDOT:PSS) (from H.C. Starck) is used as the hole injection layer and LiF as electron injection layer. PEDOT:PSS and organic compounds are sequentially spin coated on ITO glass. Then LiF and Al are thermally evaporated in vacuum. The final structure of the device has a structure of ITO/PEDOT:PSS(40nm)/ZWK1 or ZWK-2(~90nm)/LiF(1nm)/Al(100nm) and is not encapsulated.

The EL spectrum of the device is estimated in International Commission on Illumination (CIE) coordinates: x=0.65 and y=0.34 for **ZWK-1** and x=0.64 and y=0.36 for **ZWK-2**. The spectral maximum peak is observed at 667 nm and 705 nm in **ZWK-1** and **ZWK-2**, respectively, as shown in Fig.34. These peaks are slightly red shifted compared with those of PL spectrum of **ZWK-1** and **ZWK-2** thin films. This red shift may be attributed to the interaction of molecules and injected charges.

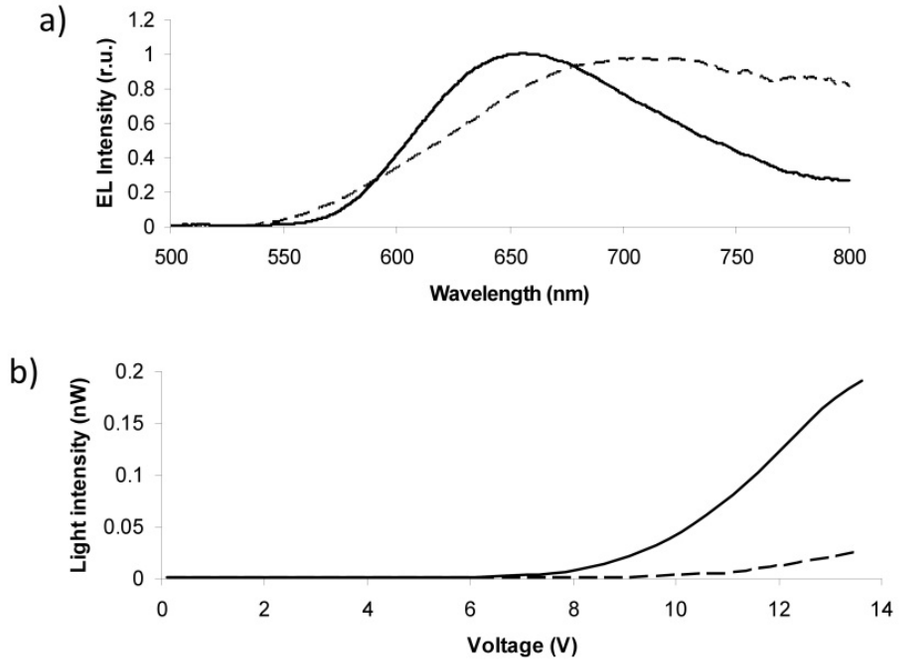

Figure 34. a) Electroluminescence spectrum and b) light intensity dependence on voltage of **ZWK-1** (line) and **ZWK-2** compounds (doted line)

The light emission is observed at 6 V in the electroluminescent device with **ZWK-1** molecules and 9 V in with **ZWK-2** molecules. The light intensity is one order less in **ZWK-2** molecules compared to that in **ZWK-1**. This may be due to the lower PLQY and shallow charge carrier trap states in **ZWK-2**.

4. Conclusions

The absorption and emission bands of the synthesized pyranylidene type compounds **ZWK-1**, **DWK-1**, **JWK-1** are comparable with those of other already known one electron donor fragment **DCM** and benzopyran type derivatives of pyranylidene within the spectral region studied here. Similar conclusions can be drawn about **ZWK-2**, **DWK-2**, **JWK-2,** which have similar properties to **IWK** and two other already known electron donnor group containing derivatives of pyranylidene. These properties are also similar to those of one electron donor fragment chromene red-emitters. However, incorporation of bulky trityloxy groups in such molecules not only enchances glass transition temperatures by 5° to 20°C compared to previously published pyranylidene type compounds containing one and two electron donor groups, but also enables the formation of a glassy structure in the solid state from volatile organic solvents. In addition, no glass transition values have been observed so far for low molecular mass isophorene type compounds. The photoluminescence quantum yield of investigated molecules in solution is up to 0.54 and is also comparable with the quantum yield of pyranylidene and isophorene derivatives already reported. Most of the thin solid films obtained from **WK-1**, **WK-2** have almost no crystals in the sample. Newertheless the photoluminescence quantum yield is reduced by one order of magnitude due to the closer intermolecular distance between molecules, resulting in strong excitonic interaction.

Emission from the **IWK** film is too weak to detect, which may be attributed to the higher photoluminescence quenching in **IWK** than in glassy pyranylidene films. However, using the doping approach, the compounds we have introduced enable up to 3 times higher doping concentration without losing optical properties compared to other already known red-emitters.

Four investigated compounds - **ZWK-1**, **JWK-2**, **DWK-1** and **DWK-2** show amplified spontaneous emission from pure solid films. Obtained threshold values are larger than those previously reported, but it should be mentioned that for pyranylidene type compounds, amplified spontaneous emission has been observed only in the doped systems until now.

Electrical properties are found to be better in compounds with one electron donor group due to absence of local trap states in their thin films. In the case of molecules with two electron donor groups shallow hole trap states have been observed, which may decrease efficiency of electroluminescence and should therefore be avoided in fabricating high efficiency light emitting diodes.

Even though we are able to prevent pyranylidene and isophorene type red-emitters from self crystallization in the solid state, their concentration in the emission layer would still be limited due to photoluminescence quenching caused by the short distance between molecules. Nevertheless, the glass materials can still be used not only as dopants for OLED applications, but also for lasing applications. Good thermal properties present a possibility of using them also for nonlinear optical (NLO) property studies.

Author details

Elmars Zarins and Valdis Kokars
Institute of Applied Chemistry, Riga Technical University, Riga, Latvia

Aivars Vembris and Inta Muzikante
Institute of Solid State Physics, University of Latvia, Riga, Latvia

Acknowledgement

This work has been supported by the European Social Fund within the project «Support for the implementation of doctoral studies at Riga Technical University» and «Support for Doctoral Studies at University of Latvia» and by Latvian State Research Programm No.2 in Materials Sciences and Information Technologies. Authors are grateful to Janis Jubles for assistance on reactant synthesis, Kristine Lazdovica for absorption and emission measurements in solutions and conducting thermogravimetric analysis, Dr. chem. Baiba Turofska for electrochemical measurements, Kaspars Pudzs for activation energy measurements, Raitis Grzibovskis for photoelectrical measurements, Dr. phys. Saulius Jursenas for photoluminescence quantum yield measurements, Dr. phys. Vidmantas Gulbinas for useful discussion and Dr. phys. Mikelis Svilans for providing language help.

5. References

[1] L.S. Hung, C.H. Chen, Recent progress on molecular organic electroluminescent materials and devices. Mater. Sci. Eng:R, 39, 143-222, (2002).
[2] P. Strohriegel, J.V. Grazulevicius, Charge-transporting molecular glasses. Adv. Mater., 14, 1439-1452, (2002).
[3] D.M. Bassani, L. Jonusauskaite, A. Lavie-Cambot, N.D. McClenaghan, J.L. Pozzo, D. Ray, G. Vives, Harnessing supramolecular interactions in organic solid-state devices: Current status and future potential. Coord. Chem. Rev., 254, 2429-2445, (2010).
[4] Y. Shirota, Y. Kuwabara, D. Okuda, R. Okuda, H. Ogawa, H. Inada, T. Wakimoto, H. Nakada, S. Yonemoto Y, Kawami, Starburst molecules based on π-electron systems as materials for organic electroluminescent devices. J. Lumin., 72-74, 985-991, (1997).
[5] L. Yang, M. Guan, D. Nie, B. Lou, Z. Liu, Z. Bian, J. Bian, C. Huang, Efficient, saturated red electroluminescent devices with modified pyran-containing emitters. Opt. Mater., 29, 1672-1679, (2007).
[6] G. Kwak, S. Wang, M.S. Choi, H. Kim, K.H. Choi, Y.S. Han, Y. Hur, S.H. Kim, 2D-π-A type Pyran based Dye Derivatives: Photophysical Properties Related to Intermolecular Charge Transfer and their Electroluminiscence Application. Dyes and Pigments. 78, 25-33, (2008).
[7] Y.S. Yao, J. Xiao, X.S. Wang, Z.B. Deng, B.W. Zhang, Starburst DCM-Type Red-Light-Emitting Materials for Electroluminescence Applications. Adv. Funct. Mater., 16, 709-718, (2006).
[8] C.Q. Ma, Z. Liang, X.S. Wang, B.W. Zhang, Y. Cao, L.D. Wang, Y. Qiu, A novel family of red fluorescent materials for organic light-emitting diodes. Synth. Met., 138, 537-542, (2003).
[9] F.G. Webster, W.C. McColgin, US patent 3 852 683, (1974).
[10] C.W. Tang, S.A. VanSlyke, C.H. Chen, Electroluminescent of doped organic film. J. Appl. Phys., 65, 3610-3616, (1989).
[11] C.H. Chen, C.W. Tang, J. Shi, K.P. Klubek, Recent developments in the synthesis of red dopants for Alq3 hosted electroluminescence. Thin Solid Films, 363, 327-331, (2000).
[12] Y.J. Chang, T.J. Chow, Highly efficient red fluoroscent dyes for organic light-emitting diodes. J. Mater. Chem., 21, 3091-3099, (2011).
[13] S. Wang, S.H. Kim, New solvatohromic merocyanine dyes based on Barbituric acid Meldrum's acid. Dyes and Pigments, 80, 314-320, (2009).
[14] D.U. Kim, S.H. Paik, S.H. Kim, Y.H. Tak, Y.S. Han, S.D. Kim, K.B. Kim, H.J. Ju, T.J. Kim, Electro-optical characteristics of indandione-pyran derivatives as red emission dopants in electroluminescent device. *Materials Science and Engineering: C,* 24, 147-149, (2004).
[15] C. Jianzhong, H.J. Suh, S.H. Kim, Synthesis and properties of conjugated copolymers with 2-pyran-4-ylidene malononitrile. Dyes and Pigments. 68, 75-77, (2006).
[16] D.H. Hwang, J.D. Lee, M.J. Lee, C. Lee, Organic light-emitting diode using a new DCM derivative as an efficient orange-red doping molecule. Curr. Appl. Phys., 5, 244-248, (2005).

[17] R. Andreu, L. Carrasquer, J. Garin, M.J. Modrego, J. Orduna, R. Alicante, B. Vilcampa, M. Allian, New one- and two-dimensional 4*H*-pyranylidene NLO-phores. Tetrahedron Lett., 50, 2920-2924, (2009).

[18] R. Andreu, S. Franco, E. Galịn, J. Garin, M.N. De Baroja, C. Momblona, J. Orduna, R. Alicante, B. Villacampa, Isophorone- and pyran-containing NLO-chromophores: a comparative study. Tetrahedron Lett., 51, 3662–3665, (2010).

[19] S. Wang, S.H. Kim, Photophysical and electrochemical properties of D-π-A type solvatofluorchromic isophorone dye for pH molecular switch. Curr. Appl. Phys., 9, 783-787, (2009).

[20] D.Y. Do, S.K. Park, J.J. Ju, S. Park, M.H. Lee, Nonlinear optical polyimides with various substituents on chromophores: synthesis and glass transition temperature. Opt. Mater., 26, 223-229, (2004).

[21] P.J. Kim, O.P. Kwon, M. Jazbinsek, H. Yun, P. Gunter, The influence of pyrrole linked to the π-conjugated polyene on crystal characteristics and polymorphism. Dyes and Pigments, 86, 149-154, (2010).

[22] P.Y. Chen, Y.U. Herng, M. Yokoyama, New double graded structure for enhanced performance in white organic light emitting diode. J. Lumin., 130, 1764–1767, (2010).

[23] X.H. Zhang, B.J. Chen, X.Q. Lin, O.Y. Wong, C.S. Lee, H.L. Kwong, S.T. Lee, S.K. Wuu, A New Family of Red Dopants Based on Chromene-Containing Compounds for Organic Electroluminescent Devices. Chem. Mater., 13, 1565-1569, (2001).

[24] Z. Guo, W. Zhu, H. Tian, Dicyanomehtylene-4*H*-pyran chromphores for OLED emitters, logic gates and optical chemosensors. J. Mater. Chem., DOI: 10.1039/c2cc31581e, (2012).

[25] P. Zhao, H. Tang, Q. Zhang, Y. Pi, M. Xu, R. Sun, W. Zhu, The facile synthesis and high efficiency of the red electroluminescent dopant DCINB: A promising alternative to DCJTB. Dyes and Pigments, 82, 316–321, (2009).

[26] C.J. Huang, C.C. Kang, T.C. Lee, W.R. Chen, T.H. Meen, Improving the color purity and efficiency of blue organic light-emitting diodes (BOLED) by adding hole-blocking layer. J. Lumin., 129, 1292–1297, (2009).

[27] H. Fukagawa, K. Watanabe, S. Tokito, Efficient white organic light emitting diodes with solution processed and vacuum deposited emitting layers. Org. Electron., 10, 798–802, (2009).

[28] A. Vembris, M. Porozovs, I. Muzikante, J. Latvels, A. Sarakovskis, V. Kokars, E. Zarins, Novel amourphous red electroluminescence material based on pyranylidene indene-1,3-dione. Latvian J. Phys. Tech. Sci., 47(3), 23-30, (2010).

[29] A. Vembris, M. Porozovs, I. Muzikante, V. Kokars, E. Zarins, Pyranylidene indene-1,3-dione derivatives as an amorphous red electroluminescence material. J. Photon. Energy, 1, 011001-1-011001-8, (2011).

[30] E. Zarins, J. Jubels, V. Kokars, Synthesis of red luminescent non symmetric styryl-4H-pyran-4-ylidene fragment containing derivatives for organic light-emitting diodes. Adv. Mater. Res., 222, 271-274, (2011).

[31] E. Zarins, V. Kokars, M. Utinans, Synthesis and properties of red luminescent 2-(3-(4-(bis(2-(trityloxy)ethyl)amino)styryl)-5,5-dimethylcyclohex-2-enylidene) malononitrile for organic light-emitting diodes. IOP Conf. Ser.: Mater. Sci. Eng. 2, 012-019, (2011).

[32] A. Vembris, E. Zarins, J. Jubels, V. Kokars, I. Muzikante, A. Miasjedovas, J. Saulius, Thermal and optical properties of red luminescent glass forming symmetric and non symmetric styryl-4H-pyran-4- ylidene fragment containing derivatives. Opt. Mater., 34, 1501-1506, (2012).

[33] R.H. Wiley, C.H. Jarboe, H.G. Ellert, Substituted 3-cinnamoyl-4-hydroxy-6-methyl-2-pyrones from dehydroacetic acid. J. Am. Chem. Soc., 77, 5102-5105, (1955).

[34] I.P. Lokot, F.S. Pashkovsky, F.A. Lakhvich, A New Approach to the Synthesis of 3.6- and 5,6-DIalyl Derivatives of 4-Hydroxy-2-pyrone. Synthesis or *rac*-Germicidin. Tetrahedron, 55, 4783-4792, (1999).

[35] M.L. Miles, C.R. Hauser, 2-(p-METOXYPHENYL)-6-PHENYL-4-PYRONE. Org. Synth. Coll., 5, 721 and 46, 60. (1973 and 1966).
http://www.orgsyn.org/orgsyn/pdfs/CV5P0721.pdf.

[36] N.S. Vulfson, E.V. Sevenkova, L.B. Senyavina, Condensation of dehydroacetic acid with aromatic aldehydes. Rus. Chem. Bull., 15(9), 1541-1546, (1964).

[37] E. Zarins, V. Kokars, A. Ozols, P. Augustovs, Synthesis and properties of 1,3-dioxo-1*H*-inden-2(3*H*)- ylidene fragment and (3-(dicyanomethylene)-5,5 dimethylcyclohex-1-enyl)vinyl fragment containing derivatives of azobenzene for holographic recording materials. Proc. of SPIE, 8074, 80740E-1-80740E- 6, (2011).

[38] C. Jianzhong, H.J. Suh, S.H. Kim, Synthesis and properties of conjugated copolymers with 2- pyran-4-ylidene malononitrile. Dyes and Pigments, 68, 75-77, (2006).

[39] Z.R. Grabowski, K. Rotkiewicz, W. Rettig, Structural Changes Accompanying Intramolecular Electron Transfer: Focus on Twisted Intramolecular Charge-Transfer States and Structures. Chem. Rev., 103, 3899-4031, (2003).

[40] V.A. Pomogaev, V.A. Svetlichnyi, A.V. Pomogaev, N.N. Svetlichnaya, T.N. Kopylova, Theoretic and Experimental Study of Photoprocesses in Substituted 4-Dicyanomethylene-4H-pyrans. High Energy Chemistry, 39, 403-407, (2005).

[41] J.C. Mello, H.F. Wittmann, R.H. Friend, An improved experimental determination of external photolumiescence quantum efficiency. Adv. Mater. 9, 230-232, (1997).

[42] P.R. Hammond, Laser dye DCM, its spectral properties, synthesis and comparsion with other dyes in the red. Opt. Commun., 29, 331-33, (1979).

[43] S.I. Bondarev, V.N. Knyukshto, V.I. Stepuro, A.P. Stupak, A.A. Turbanov, Fluorescence and Electronic Structure of the Laser Dye DCM in Solutions and in Polymethylmetacrylate. J. Appl. Spectrosc., 71, 194-201, (2004).

[44] R. Kapricz, V. Getautis, K. Kazlauskas, S. Juršenas, V. Gulbinas, Multicoordinational excited state twisting of indan-1,3-dione derivatives. Chem. Phys., 351, 147-153, (2008).

[45] V.G. Kozlov, S.R. Forrest, Lasing action in organic semiconductor thin films. Current opinion in Solid State and Materials Science 4(2), 203-208, (1999).

[46] A. Vembris, I. Muzikante, R. Karpicz, G. Sliauzys, A. Misajedovas, S. Jursenas, V. Gulbinas, Fluorescence and amplified spontaneous emission of glass forming

compounds containing styryl-4H- pyran-4-ylidene fragment. J. Lumin., 132, 2421-2426, (2012).
[47] E.M. Calzado, J.M. Villalvilla, P.G. Boj, J.A. Quintana, R. Gomez, J.L. Segura M.A. Diaz Garcia, Amplified spontaneous emission in polymer films doped with a perylediimide derivative. Appl. Optic. 46, 3836-3842, (2007).
[48] J.Y. Li, F. Laquai, G. Wegner, Amplified spontaneous emission in optically pumped pure films of a polyfluorene derivative. Chem. Phys. Lett., 478, 37-41, (2009).
[49] E.A. Silinsh, V.V. Capek, Organic Melecular Crystals. Interaction, localization and transport phenomena (AIP Press, New York), (1994).
[50] E.A. Silinsh, M. Bouvet, J. Simon, Molecular Materials 51, (1995).
[51] E.A. Silinsh, Organic Molecular Crystals Their Electronic States. Springer Series in Solid-State Sciences 16, Berlin, (1980).
[52] A. Rose, Space-Charge-Limited Currents in Solids. Phys. Rev. 97, 1538-1655, (1955).
[53] A. Rose, Concepts in Photoconductivity and Allied Problems. Interscience, New York, (1967).
[54] M.A. Lampert, P. Mark, Current Injectio in Solids. Academic Press, New York, (1970).
[55] S. Nešpůrek, O. Zmeškal, J. Sworakowski, Space-charge-limited currents in organic films: Some open problems. Thin Solid Films, 516, 8949, (2008).